

AD-785 144

OXYGEN CONCENTRATION SENSOR FOR AIR-  
CRAFT FUEL TANKS

Jean Bordeaux, et al

Beckman Instruments, Incorporated

Prepared for:

Air Force Aero Propulsion Laboratory

May 1974

DISTRIBUTED BY:

**NTIS**

National Technical Information Service  
U. S. DEPARTMENT OF COMMERCE  
5285 Port Royal Road, Springfield Va. 22151



UNCLASSIFIED

Security Classification

AD 785 144

DOCUMENT CONTROL DATA - R & D

Security Classification of title, body of abstract, & covering annotation must be entered when the overall report is classified

1. ORIGINATOR ACTIVITY (Corporate Author)		20. REPORT SECURITY CLASSIFICATION	
Beckman Instruments, Inc. Advanced Technology Operations		UNCLASSIFIED	
3. REPORT TITLE		21. GROUP	
OXYGEN CONCENTRATION SENSOR FOR AIRCRAFT FUEL TANKS		NOT APP.	
4. DESCRIPTIVE NOTES (Type of report and inclusive dates)			
Final Technology Report 1 Nov. 1972 to 5 May 1974			
5. AUTHOR Surname, first name, middle initial, last name			
6. REPORT DATE			
May, 1974		18. TOTAL NO. OF PAGES	19. NO. OF REFS
		54	NONE
8a. CONTRACT OR GRANT NO.		16. ORIGINATOR'S REPORT NUMBER(S)	
F33615-73-C-2008		FR-2653-102	
c. PROJECT NO. 3048		9f. OTHER REPORT NO(S) (Any other numbers that may be assigned this report)	
e. Task No. 304807		AFAPL-TR-74-17	
d. Work Unit - 30480746			
10. DISTRIBUTION STATEMENT			
Approved For Public Release Distribution Unlimited			
11. SUPPLEMENTARY NOTES		12. SPONSORING MILITARY ACTIVITY	
		AFAPL WPAFB, OHIO 45433	
13. ABSTRACT			
<p>The ullage in aircraft fuel tanks becomes potentially explosive when the oxygen concentration of the fuel vapor-air mixture exceeds approximately 9% by volume. To insure effective and efficient use of active fuel tank inerting under a wide range of environmental and operational conditions, the oxygen concentration must be continuously monitored. This study has resulted in the development of a laboratory breadboard model of a sensor which is specific for oxygen. The concept employs a change in frequency of a radio-frequency (RF) oscillator due to the paramagnetic property of oxygen. Demonstration of feasibility was limited to ambient laboratory conditions.</p>			

Report available by  
**NATIONAL TECHNICAL  
INFORMATION SERVICE**  
U.S. Department of Commerce  
Springfield, MA 01104

DD FORM 1473

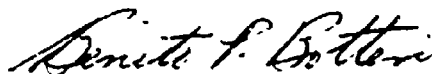
UNCLASSIFIED

Security Classification

## FOREWORD

This is the final Technical Report prepared and submitted by Advanced Technology Operations of Beckman Instruments, Inc. The effort was sponsored by the Air Force Aero Propulsion Laboratory, Air Force Systems Command, Wright-Patterson AFB, Ohio under Contract No. F33615-73-C-2008 for the period 1 November 1972 to 1 May 1974. The work herein was accomplished under Project 3048 "Fuels, Lubrication, and Fire Protection", Task 304807, "Aerospace Vehicle Fire Protection" with G.T. Beery, AFAPL/SFH, as Project Engineer. Mr. Jean Bordeaux of Beckman Instruments, Inc. was technically responsible for the work. Other Beckman personnel were: M. W. Green, Scientist; Wallace Chase, Chief Project Engineer; John Fisher, Mechanical Engineer.

This technical report has been reviewed and is approved.



Benito P. Botteri  
Chief, Fire Protection Branch  
Fuels and Lubrication Division

## ABSTRACT

A technique for measuring the percent of oxygen in the ullage space of an aircraft fuel tank was selected for laboratory investigation to determine the feasibility of the technique. Available oxygen sensing systems are not designed for the application nor the environment and as such cannot be directly applied to the problem.

A measurement concept based on the unique paramagnetic property of the oxygen molecule was selected. Analyses of several possible methods of utilizing the paramagnetic property for sensing oxygen concentration were made. Calculations showed that the most promising approach was to use an oscillating circuit wherein the resonant frequency of the circuit would vary in proportion to oxygen concentration. This was accomplished by placing an air core inductor in a sampling chamber so that the coil inductance would be changed as a result of the influence of oxygen on the flux field around the coil. This resulted in a frequency change of the LC circuit. Oxygen concentration was quantitized by beating the LC circuit output against a stable clock frequency. The difference in frequency is a direct measure of the partial pressure of oxygen in the sampling chamber.

A series of tests were made at room temperature on two breadboard assemblies. Oxygen measurements were made from 0 to 100%. Accuracy of the measurement was limited by system noise which was equivalent to about 2% oxygen. Noise sources were identified as well as areas for improving signal strength so that it was concluded that measurements approaching 1% of true value could very likely be achieved with further work. The noise sources were discussed and a plan for eliminating them was presented along with high temperature testing in the presence of fuel vapors.

TABLE OF CONTENTS

PARAGRAPH		PAGE
1.0	INTRODUCTION AND SUMMARY . . . . .	1
1.1	The Need for Measuring Oxygen in Aircraft Fuel Tanks and the Difficulties Involved . . . . .	1
1.2	Inability of Available Oxygen Sensors to Meet Requirements . . . . .	1
1.3	Summary of Contract Objectives and Work Accomplishments . . . . .	3
1.4	Features and Performance Obtained from Laboratory Breadboard RF Sensor . . . . .	4
2.0	ANALYTICAL STUDIES . . . . .	6
2.1	Evaluation of Greene-Hummel Approach . . . . .	6
2.1.1	Summary of Modified Greene-Hummel Principle of Operation and Potential Performance Capability. . . . .	6
2.1.2	Difficulty in Selection of Chopper Materials and Design of Chopper to Attain Required Performance . . . . .	8
2.1.3	Impact of Pickup Coil and Preamplifier Noise on S/N . . . . .	10
2.1.4	Impact of Preamplifier Bandpass Requirement of Preamplifier Noise. . . . .	12
2.2	Alternative Designs . . . . .	14
2.2.1	Evaluation of the Hornfeck Multiple Pole Approach . . . . .	14
2.2.2	Evaluation of the Rotating Magnetic Field Concept . . . . .	16
2.2.3	Rationale for Selection of the RF Over the Greene- Hummel Approach . . . . .	17
3.0	SYSTEM DESCRIPTION . . . . .	18
3.1	Overall System Description . . . . .	18
3.2	Electronics . . . . .	19
3.2.1	Overall Electronics Design . . . . .	19
3.2.2	Functional Description of the Measurement Oscillator . . . . .	19
3.2.3	Calculation of System Resolution . . . . .	26
3.3	Mechanical . . . . .	27
3.3.1	Details of the Mechanical Design . . . . .	27
4.0	TEST RESULTS . . . . .	29
4.1	Static Tests . . . . .	29
4.1.1	Testing to Determine How to Achieve Maximum Inductance . . . . .	29
4.1.2	Testing the Chopper to Determine Positioning and Timing Accuracy . . . . .	30
4.2	Functional Tests (MOD 1) . . . . .	31
4.2.1	Test Results for the MOD 1 Configuration . . . . .	31
4.2.2	Noise Sources Related to Output Counts and Frequency Changes . . . . .	33
4.2.3	Measurement of Electronic Noise with Chopper not Moving. . . . .	34
4.2.4	Investigation of Noise and Drift From Chopper Operation. . . . .	36
4.2.5	Effects of Screen and Metallic Crankshaft Modulations on Baseline Drift and Noise Level. . . . .	37

TABLE OF CONTENTS (Continued)

PARAGRAPH		PAGE
4.3	Functional Tests (MOD II) . . . . .	40
4.3.1	Overall Performance of the MOD II . . . . .	40
4.3.2	Detail Results and Interpretation of Gas Sample Tests . . . . .	43
5.0	CONCLUSIONS AND RECOMMENDATIONS . . . . .	45
5.2	Discussion of Recommended Development Program . . . . .	45

## LIST OF FIGURES

### FIGURE NO.

- 1 MOD II Laboratory Breadboard Model
- 2 Diamagnetic Susceptibility of Hydrocarbons Showing Linear Relation to Number of Carbons, and the Effect of Multiple Carbon Bonds
- 3 Temperature Coefficient of Susceptibility of Chopper Formed of Mixture of Diamagnetic and Para-magnetic Components
- 4 Output of Pickup Coil Assumed for Computer Analysis of Preamplifier Bandpass Requirements
- 5 Hornfeck Multiple Pole Approach
- 6 Rotating Magnetic Field Concept--End View
- 7 Configuration of MOD I Laboratory Breadboard Model
- 8 Configuration of MOD II Laboratory Breadboard Model
- 9 Overall Electronic Design of Oxygen Fuel-Tank Sensor
- 10 Bandpass Filter
- 11 Digital Electronics
- 12 Digital-to-Analog Converter
- 13 Electronic Schematic Diagram of Measurement Oscillator
- 14 Mechanical Configuration of Aircraft Fuel Tank O<sub>2</sub> Sensor
- 15 MOD II--Internal Parts
- 16 MOD I--Sample Gas Tests
- 17 MOD I--Electronic Noise Only (Chopper Off)
- 18 MOD II--Electronic Noise Only (Chopper Off)
- 19 MOD II--Stability Test Measuring Room Air
- 20 MOD II--Response to Cycled Sample Gas

## 1.0 INTRODUCTION AND SUMMARY

### 1.1 The Need for Measuring Oxygen in Aircraft Fuel Tanks and the Difficulties Involved

The ullage in aircraft fuel tanks contains an explosive fuel vapor-air mixture when the oxygen concentration exceeds about 9% by volume. To enable effective use of inerting systems, the oxygen concentration must be measured under environmental extremes that preclude the use of commercial instruments.

Aircraft presently operate with potentially explosive mixtures in the ullage (gas space) of the fuel tanks. At least one commercial aircraft has been lost due to detonation of the combustible fuel vapor-air mixture in the fuel tanks by lightning. Military transports are subject to additional sources of damage such as small arms fire. Inerting systems are being developed to prevent the occurrence of explosive conditions (i.e., above 9% oxygen by volume in the ullage of the fuel tanks).

To be effective, an inerting system must prevent the concentration of oxygen from ever exceeding about 9% by volume in the ullage space. For higher oxygen concentrations, a spark of sufficient energy can cause an explosion of the fuel vapor-air mixture. For oxygen concentrations below about 9% by volume, the mixture cannot explode; that is, a flame is not self-propagating. Clearly, it is desirable to have an oxygen sensor capable of directly and continuously monitoring the concentration of oxygen in the ullage to verify that the inerting system is performing correctly.

To directly measure oxygen in the ullage of a fuel tank, the oxygen sensor must perform accurately and reliably under severe environmental conditions. Commercially available oxygen sensors cannot meet most of these requirements (see Table 1).

### 1.2 Inability of Available Oxygen Sensors to Meet Requirements

All commercially developed oxygen sensing techniques were surveyed and found incapable of meeting one or more of the basic requirements for the fuel-tank environment. Only the commercially undeveloped Greene-Hummel approach seemed capable of meeting the requirements.

A brief survey of available oxygen sensors was required to select the most promising approach for an optimum fuel-tank sensor. Beckman Proposal CS73-501, submitted in response to RFQ F33615-73-Q-2008, contains a relatively detailed discussion of the available sensors and an analysis of their suitability for this application. A summary of the deficiencies of each approach is given in Table II. The sensors considered were:

- Electrochemical sensors, variously called polarographic, galvanic, or fuel cells. All have a diffusion limiting, gas permeable membrane over the cathode.

Table I. Comparison of Operational Requirements for Fuel-Tank Oxygen Sensor with Operating Parameters of Commercial Instruments

<u>Operational Requirements</u>	<u>Commercial Instrument Typical Parameters and Characteristics</u>
● Operating Temperature: -54 to 170°C	- 0 to 50°
● Operating Pressure: 2 to 25 psig, dynamic	- Pressure stable to within ±1%
● Specificity: maintain calibration with variations of N <sub>2</sub> , CO <sub>2</sub> , and fuel vapor content	- Specificity varies
● Readout: Direct 0-15% O <sub>2</sub> by volume output	- Partial pressure O <sub>2</sub> output
● Fuel-wetting: no detrimental effect from submersion	- Liquids prohibited
● Repeatability: 1% of full scale for any 90-day period	- 1% for 24 hours
● Response Time: not to exceed one minute for any combination of conditions	- Inoperative under some conditions

Table II. Summary of Deficiencies of the Available Techniques Surveyed

Electrochemical

- Cannot meet thermal requirements

Ultraviolet Absorption

- Cannot operate after fuel wetting
- Fuel vapor interface would probably be large

Indirect Paramagnetic

- Cannot meet specifications due to large and complicated dependence upon temperature, pressure, orientation, and background gas

Direct Paramagnetic

- Viscosity bridge cannot meet thermal or fuel wetting requirements
- Beckman/Pauling sensor cannot meet fuel wetting requirements
- Greene-Hummel approach appeared capable of meeting all major requirements, but had never been commercially developed

- Spectrophotometer, ultraviolet absorption by oxygen in the 140- to 150-nanometer region.
- Indirect paramagnetic sensors, utilizing combined thermal and magnetic effects.
- Direct paramagnetic sensors, including the viscosity bridge, Beckman/ Pauling torsion balance, and the Greene-Hummel Reluctance sensor. The Greene-Hummel sensor has never been commercially developed.

Of these known approaches, only the Greene-Hummel sensor appeared capable of meeting all basic requirements.

### 1.3 Summary of Contract Objectives and Work Accomplishments

The major objective of selecting an optimum technique to measure oxygen concentration in the ullage of an aircraft fuel tank has been accomplished. The feasibility of the technique has been demonstrated by testing a laboratory breadboard model and measuring low concentrations of oxygen. However, testing was limited to ambient conditions and needs to be extended to determine performance in simulated environments.

The basic contract objectives were to select one approach capable of development into an optimum fuel-tank oxygen sensor and to design, fabricate, and test a breadboard model of the sensor in simulated tanks to demonstrate compliance with the basic environmental and performance requirements.

Based upon the review of available techniques described in Beckman proposal CS73-501, the Greene-Hummel approach was selected for detailed design analysis. The program plan called for a complete analysis of the Greene-Hummel sensor to verify that the performance predicted in the proposal could be achieved. The program plan then called for generation of detail designs, fabrication, and testing.

Major difficulties arose as the Greene-Hummel sensor analysis proceeded. As a consequence, several alternative configurations were considered. Approximately three months of effort were devoted to analyzing these alternatives. Over two hundred pages of calculations were submitted to Wright-Patterson, along with our recommendation to abandon the basic Greene-Hummel approach in favor of measurement of the resonant frequency of a coil, such frequency being a function of the magnetic susceptibility of the medium surrounding the coil. This approach, called the "RF Sensor" for brevity, was subsequently designed, fabricated, and tested.

The following paragraph summarizes the features and performance of the laboratory model of the RF Sensor.

#### 1.4 Features and Performance Obtained from Laboratory Breadboard RF Sensor

Based upon tests at ambient conditions only, the RF Sensor has demonstrated the potential to meet all basic requirements of the application. Only minor rework of mechanical parts and re-tuning with high-temperature-resistant electronics should be required to permit operation at 170°C (controlled) before testing in a fuel tank can be accomplished.

The final laboratory breadboard model of the RF Sensor (MOD II), shown in Figure 1, consisted of a sampling chamber, a radio-frequency (RF) oscillator, a zero reference chopper, a reference crystal oscillator, and a chopper actuator. Its features and potential performance are summarized below:

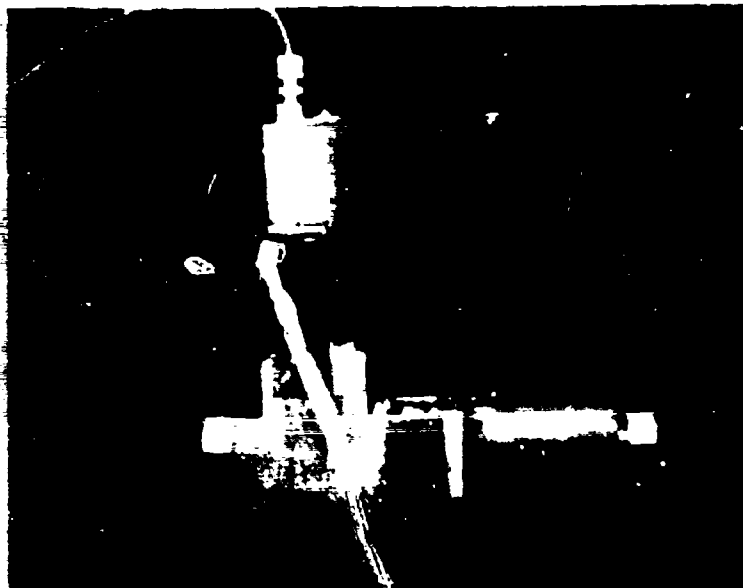


Figure 1. MOD II Laboratory Breadboard Model

- Concept Feasibility  
The measuring concept described is sufficiently sensitive to use the paramagnetic property of oxygen as a means of quantifying low concentrations of oxygen.
- Dynamic Range  
A dynamic range capability of from 0 to 15% oxygen can be provided.

- Accuracy  
An absolute accuracy of 0.5% is possible over the entire dynamic range from a minimum level of 5% oxygen. From 0 to 5%, a 1% accuracy is possible.
- Readout Interval  
While sampling would be done on a continuous basis, oxygen concentration readouts are possible at 10-second intervals.
- Readout  
Pressure compensation can be accomplished to provide a direct meter readout in percent oxygen by volume. This could cover the range of from 2 to 35 psia.
- Wetting Impact  
The pressure of jet fuel vapors, carbon dioxide, or nitrogen will not interfere with the oxygen measurements.
- Safety  
The sensor would not constitute an ignition source or other hazard in the fuel tank.
- Noise Level  
Noise levels could be reduced with improved electronic and mechanical design to the point that 1% resolution is possible in the 0 to 9% oxygen-by-volume range.
- Temperature Range  
Although elevated temperature tests were not made, from our analyses we have concluded the system should be capable of operating at 170°C with available components.
- Replenishables  
No replenishables are necessary for the system.
- Power Supply  
The system can be made to operate from available aircraft power supplies.
- Power Consumption  
Total power consumption should not exceed 10 W during continuous operation. The sensor head would take a major portion of this, so that higher wattages would be necessary for accelerated warmup from low ambient temperatures.
- Weight and Volume  
A flight model sensor head should not exceed 5 lb in weight. Supporting electronics should not exceed 10 lb and should easily be contained in a standard 19-inch rack mounting.

- Stability, Maintenance, Calibration

Breadboard tests were not sufficient to predict long-term stability, maintenance, or calibration requirements.

2.0 ANALYTICAL STUDIES

2.1 Evaluation of Greene-Hummel Approach

2.1.1 Summary of Modified Greene-Hummel Principle of Operation and Potential Performance Capability

The Greene-Hummel magnetic reluctance principle was selected for detailed study because it was the only technique that appeared capable of meeting all of the basic requirements for an aircraft fuel-tank oxygen sensor.

Advantages of the Approach--The Greene-Hummel approach is based upon the effect of oxygen upon the reluctance of a magnetic circuit. The principle had been described first by W. J. Greene and then by Dr. Heinz Hummel. In 1958 a prototype Hummel sensor was fabricated at Beckman that operated within the expected parameters. Although low signal levels were typical of the Greene-Hummel type of sensor, it had several advantages of importance to oxygen measurement in the ullage of fuel tanks; it was entirely free from contamination problems, it was rugged, it would clear itself if wetted with fuel, and it was capable of operating over very wide temperature and pressure ranges (see Table III). Other approaches did not offer this combination of advantages. Consequently, the Greene-Hummel approach was considered to be the only technique with the capability of meeting the requirements for an aircraft fuel-tank sensor.

Table III. Comparison of Required Specifications and Potential Capability of Modified Greene-Hummel Sensor

Required Operating Parameter and Range	Potential Capability Based Upon Materials and Theory of Operation of Greene-Hummel Sensor
● -54 to 170°C	- -65 to +200°C
● 2 to 25 psig, dynamic	- Can be compensated with two pressure transducers
● Specific to oxygen	- Satisfactory
● Direct % O <sub>2</sub> output	- Satisfactory (2 transducers)
● Immune to fuel wetting	- Transient effects only
● 1% repeatability for 90 days	- Theoretically possible
● No sample conditioning	- None required

Principle of Operation--The measurement of oxygen by the Greene-Hummel technique is based upon the fact that oxygen is highly paramagnetic (i.e., attracted into a region of higher magnetic field) compared to other gases of concern, which are slightly diamagnetic (i.e., expelled from a magnetic field). In particular, the hydrocarbons of fuel vapor have small and predictable magnetic susceptibilities (see Figure 2). Thus, the Greene-Hummel technique was considered sufficiently specific for oxygen within the required operating environment.

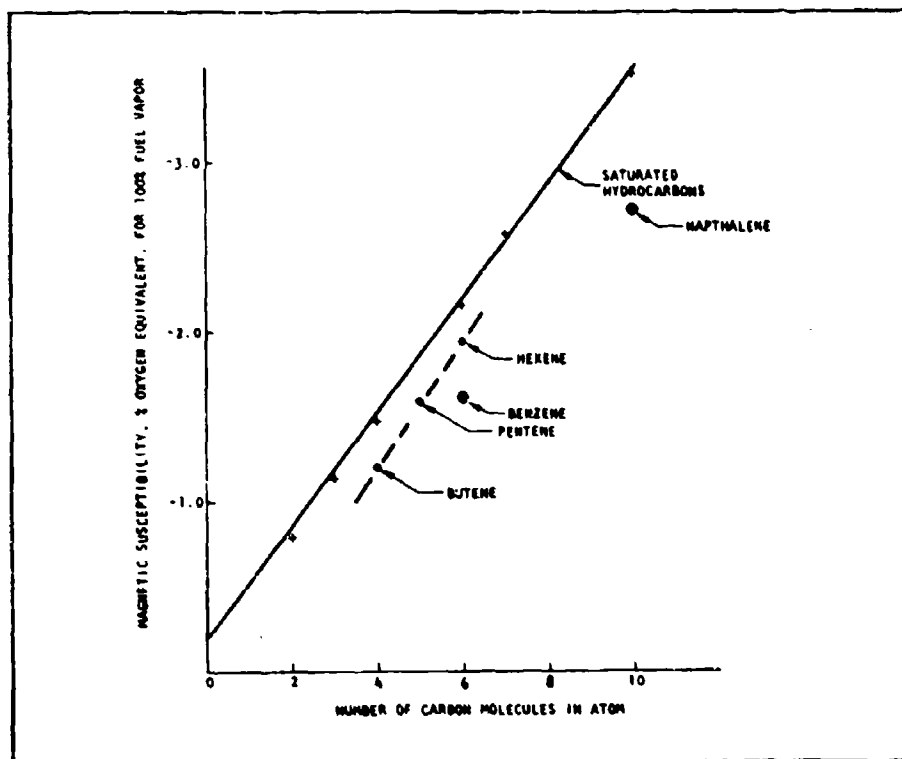


Figure 2. Diamagnetic Susceptibility of Hydrocarbons Showing Linear Relation to Number of Carbons, and the Effect of Multiple Carbon Bonds

The modified Greene-Hummel sensor measures the susceptibility of the sample by alternately introducing sample gas and two solid references into the air gap of a magnetized magnetic structure. The chopper sequence would be zero-sample-zero-reference-zero-etc. The change in magnetic flux linking a coil located on the magnetic structure due to the changes in the magnetic reluctance of the air gap induces an alternating voltage in the pickup coil, the amplitude of which is proportional to the difference between the zero reference and the sample susceptibility for one cycle, and to the difference between the zero and upscale reference susceptibilities for the following cycle. These portions of the total cycle are synchronously demodulated to provide separate dc analog signals proportional to the sample and reference susceptibilities, respectively.

The resultant dc signals may be ratioed electronically to cancel all common-mode sources of error, such as variations in magnetic field strength, air-gap length and area, magnetic core permeability, and the effects of a liquid fuel film coating the pole faces and the chopper.

The ratioed output may be further compensated for the effects of temperature and pressure upon both the output zero and sensitivity of the system. The compensated output may then be divided by the output of an absolute pressure transducer to convert the final output to the required percentage-of-oxygen basis.

Conclusion--All materials of construction are capable of withstanding the fuel-tank environment, but further evaluation of this approach was necessary before an optimum sensor of this type could be designed. The major factors requiring further study were chopper materials and chopper mechanical design, weight versus sensitivity tradeoffs, and optimization of the signal-to-noise ratio.

#### 2.1.2 Difficulty in Selection of Chopper Materials and Design of Chopper to Attain Required Performance

A detailed study of chopper materials revealed that the sensor output zero dependence upon temperature would be about 100 times as large as the initial estimate. This fact made the precise compensation originally proposed virtually impossible unless a more complex chopper and demodulation scheme could be employed.

Assumptions Re Susceptibility of Ideal Chopper Material--Idealized implementation of the Greene-Hummel approach described in Subsection 2.1.1 assumed that the chopper base material had a diamagnetic susceptibility equivalent to minus a few percent oxygen (STP), and that the zero and up-scale reference could be obtained by adding different amounts of a slightly paramagnetic salt to this low susceptibility base material. This assumption was based upon handbook data indicating that beryllia (BeO) had very low susceptibility. The study revealed that published values merely reflect the purity of the material tested, and that all pure diamagnetic materials have roughly the same susceptibility. Furthermore, the susceptibility of materials useful for chopper construction is of the order of minus 500% O<sub>2</sub> (STP) equivalent.

Data Re Susceptibility of "Real" Chopper Materials--The large diamagnetic susceptibility for "real" chopper materials as opposed to the idealized chopper means that a real chopper will have a large thermal coefficient of susceptibility. It can be made to have zero susceptibility by the addition of a paramagnetic salt at only one temperature. The diamagnetic solid has virtually no thermal coefficient, and the paramagnetic solid's susceptibility varies inversely with absolute temperature. If both susceptibility components are small compared to full-scale oxygen, the effect may be compensated with acceptable precision. However, a chopper having a zero-reference susceptibility obtained by a combination of diamagnetic and paramagnetic materials equivalent to minus and plus 500% O<sub>2</sub> at standard temperature and pressure (STP) at 25°C will have a net susceptibility of about -160% O<sub>2</sub> at 170°C and +180% O<sub>2</sub> at -54°C. The required full-scale range of 15% O<sub>2</sub> (STP) means that the zero and upscale reference could change about ±10 times full scale over the -54°C to 170°C range. Accurate compensation of the output would, therefore, require

impractically precise temperature measurement. The situation is illustrated in Figure 3.

- A - Idealized chopper, with each component equivalent to full-scale oxygen (15%) at 25°C.
- B - Probable coefficient for real alumina or beryllia chopper with each component equivalent to 33 times full-scale oxygen (500%) at 25°C.

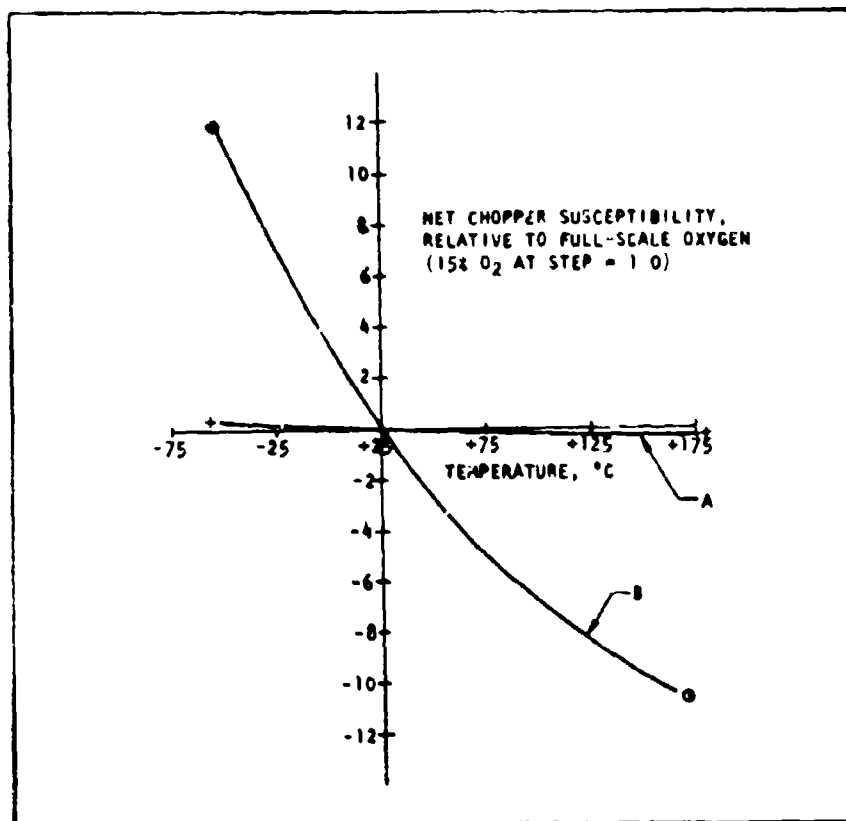


Figure 3. Temperature Coefficient of Susceptibility of Chopper Formed of Mixture of Diamagnetic and Paramagnetic Components

Possible Solutions to Chopper Susceptibility Problems--There are several possible ways of reducing the error caused by the larger chopper material susceptibility. They are:

- Use of hollow zero and up-scale reference segments to reduce the number of molecules inserted in the gap by a factor of about ten. However, gating of the preamplifier to block the large transients introduced by solid chopper chamber walls would be necessary in

this case. Chopper design and fabrication would be difficult, but preliminary calculations indicate that the strength would be adequate.

- Use of a ferromagnetic additive having a very low temperature coefficient of permeability instead of a paramagnetic additive could reduce the net chopper temperature coefficient. This approach would require precise addition of parts per million of ferromagnetic material.
- Control of sensor temperature at 170°C, which is possible but sacrifices one of the major advantages of the Greene-Hummel sensor originally believed to be achievable.

Mechanical Design Problems--The chopper mechanical design requirements were also reviewed. While the chopper disc would be fragile, both alumina and beryllia should withstand the rotational stresses. The mechanical tolerances would be quite severe. For example, the shaft and chopper blade should be very perpendicular, with an allowable tolerance of about 0.001 inch (per inch along the radius) wobble of the disc. Fabrication of a chopper with hollow reference chambers appeared to be feasible, but it was apparent that a significant development program beyond the scope of this contract would have been required. A rotating magnet version, discussed in Subsection 2.2.2, has some advantages in this regard.

Conclusion--In summary, the study revealed that a practical chopper at reasonable cost would have such a large thermal coefficient of susceptibility that it would be necessary to control the sensor temperature at 170°C. One of the major anticipated advantages of the Greene-Hummel approach could not, therefore, be realized within the scope of this contract. This was a major factor leading to the ultimate selection of the RF sensor (which also requires temperature control) for the laboratory model.

### 2.1.3 Impact of Pickup Coil and Preamplifier Noise on S/N

Preamplifier input current and voltage noise limit the signal-to-noise ratio (S/N) attainable with a sensor of given mass. Within a given mass restraint, the S/N can be optimized by proper selection of chopping frequency, coil resistance and inductance, and other design parameters.

The optimization of S/N by control of design tradeoffs was a major goal of the analytical studies. In particular, it was necessary that all feasible means of improving the magnitude of the signal be evaluated from the standpoint of their impact upon noise, since the basic goal was improvement of S/N (see Table IV). Briefly stated, this study indicated that while S/N could be optimized by selection of design parameters, the limiting S/N for a sensor of about five pounds would be marginal, and would be set by the input voltage and current noise parameters of the preamplifier.

Preamplifier Voltage Noise--The most fundamental parameter is the input voltage noise,  $E_n$ , of the preamplifier, because no design parameters affect this noise source (except amplifier temperature). The net noise is the square root of the sum of the squares of the individual noise component amplitudes. Completely

Table IV. Summary of Impact of Electronic Noise Sources

Preamplifier voltage noise

- Most fundamental parameter, since it cannot be influenced by design parameters (except operating temperature). Optimum system S/N occurs when other sources are equal to or less than amplifier voltage noise.

Preamplifier current noise

- Resistive component can be made negligible.
- Capacitive component is negligible at useful chopper frequencies.
- Inductive component sets maximum limits upon number of coil turns and chopper frequency.

Johnson noise

- Can be made negligible compared to amplifier noise.

Interconnecting cable

- Not feasible; preamplifier must be located in sensor.

eliminating Johnson noise,  $J_n$ , and the noise generated by the preamplifier input current noise,  $I_n$ , will make the system noise proportional to  $E_n$ . Reducing  $J_n$  and  $I_n$  generated noise so that each is equal to  $E_n$  will only increase total noise by the square root of 3, or 1.7. In optimizing the design parameters that affect both signal and noise, therefore, it is practical to make the other noise components equal to the noise from the  $E_n$  component.

Preamplifier Current Noise--The preamplifier input current noise,  $I_n$ , generates an equivalent voltage noise,  $e_n$ , which is the product of  $I_n$  and the input impedance,  $Z_n$ . The pickup coil impedance is complex, consisting of coil resistance, capacitance, and inductance. The equivalent voltage noise,  $e_n$ , includes, therefore, resistive,  $e_r$ , and reactive,  $e_c$  and  $e_l$ , components. The inductive component,  $e_l$ , increases with frequency, which is a factor making the preamplifier noise as well as the signal dependent upon chopper frequency,  $\omega$ .

The inductive component is also proportional to coil inductance,  $L$ , which increases with the square of the number of coil turns. Signal, however, increases at a linear rate with the number of turns, which means that for a given chopper frequency there will be a maximum S/N as the number of turns is increased. The maximum S/N occurs when the inductive current noise component,  $e_l = \omega LI_n$ , equals the preamplifier voltage noise.

The capacitive component,  $e_c$ , is negligible for frequencies significantly lower than the resonant frequency of the coil, which is a necessary condition for other reasons. The resistive component,  $e_r$ , is not frequency dependent. It may be made negligible compared to  $e_L$  by selection of a coil wire size that will make the coil resistance,  $R$ , negligible compared to  $\omega L$ . The other factors affecting coil resistance--pole size, number of turns, length of coil, and coil temperature--must also be considered in the selection of wire size.

Johnson Noise--The Johnson noise,  $J_n$ , is proportional to the square root of the coil impedance. Calculations indicate that for a practical sensor with a solid-state preamplifier, the Johnson noise will be negligible compared to the amplifier current generated noise,  $e_n$ .

Effect of Pole Area on Noise--For a given magnetomotive force, both the signal and the inductive component of noise,  $e_L$ , increase linearly with pole area. This means of increasing signal is preferred over increasing the number of turns,  $N$ , since  $e_n$  increases as  $N^2$ , while the signal increases linearly with  $N$ . Pole area should, therefore, be maximized for a given sensor mass.

Maximizing the Magnetomotive Force--Once the design parameters are optimized, as briefly discussed above, the only means of improving S/N is to increase the magnetomotive force to increase the flux in the gap. Maximizing the magnetomotive force for a sensor of given mass is, therefore, desirable. However, it must be noted that the maximum useful magnetomotive force is determined by the allowable flux density for the core material, and also by the value of the incremental permeability of the material when operating at maximum flux density. It is the product of the two which must be maximized.

Interconnecting Cable Noise--Finally, it should be noted that the use of an interconnecting cable does not appear to be feasible because of cable-generated noise. It was concluded that the preamplifier must be located within the sensor.

Discussed next is the required preamplifier bandwidth, which is an important factor in connection with preamplifier noise.

#### 2.1.4 Impact of Preamplifier Bandpass Requirement of Preamplifier Noise

The preamplifier bandpass requirement was found to be much more severe than it was originally believed to be. The major impact was to lower the S/N in the preamplifier, setting a maximum limit upon preamplifier gain.

##### 2.1.4.1 Derivation of Required Bandpass

Computer simulation was employed to determine the harmonic content, and hence the required preamplifier bandpass, of the semi-sinusoidal waveform expected from the sensor pickup coil. Typical signal waveforms for two conditions are shown in Figure 4. When the reference and sample waveforms are of equal amplitude, the harmonic content is low, but for zero oxygen it was shown that there was significant content (0.37%) out to the 21st harmonic. For a bandwidth which included only the fifth harmonic, the computer reconstruction indicated peak amplitudes of +8 and -4% would be seen instead of zero in the zero oxygen interval.

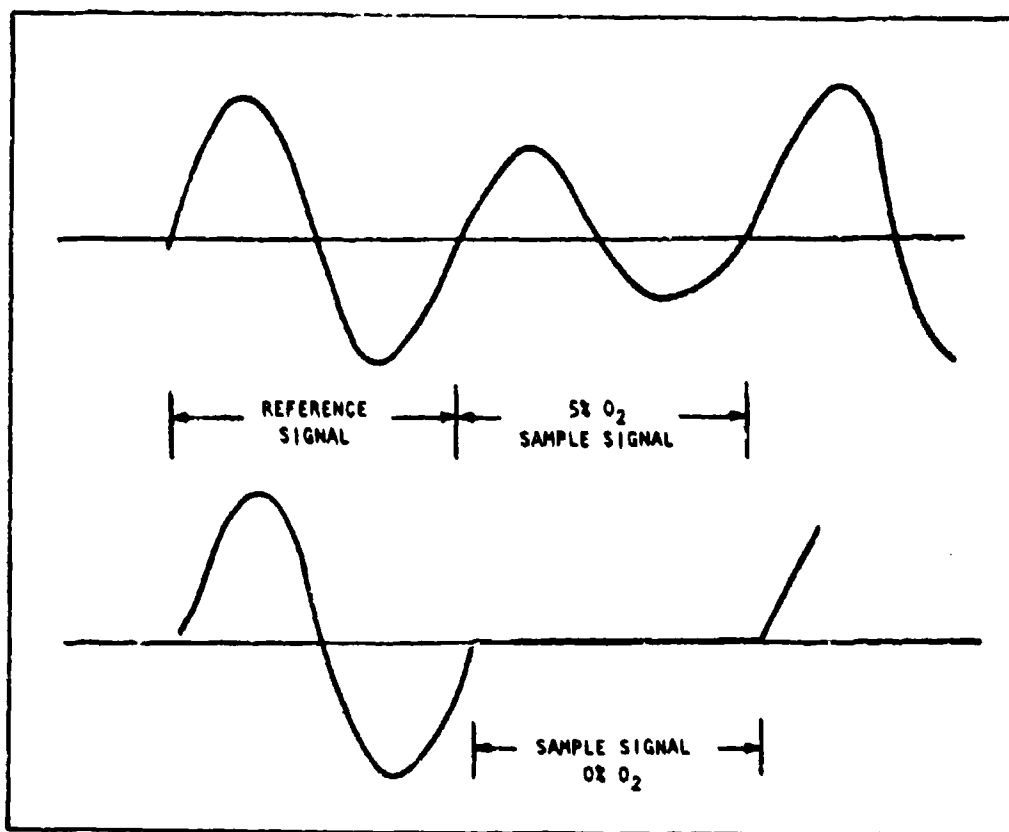


Figure 4. Output of Pickup Coil Assumed for Computer Analysis of Preamplifier Bandpass Requirements

Since the true output could be expected to be much more complicated than that assumed (Figure 4), it is probable that the bandpass requirements would have been more severe than those for the assumed waveform. It was therefore concluded that the preamplifier bandpass should be at least ten times the chopper-generated fundamental frequency to avoid significant crosstalk between reference and sample cycles.

#### 2.1.4.2 Impact of the Determined Bandwidth

The major impact of preamplifier bandwidth is upon the total rms noise, which increases as the square root of the bandwidth. The preamplifier gain must be such that peak noise is not clipped if the noise is to be successfully eliminated by reducing the bandpass after demodulation. Since a typical solid-state preamplifier can provide  $\pm 10$  V output without clipping, the peak noise must not exceed 10 microvolts if the gain is to be one million. Sample calculations for a five-pound sensor indicated that preamplifier noise of less than 0.5 microvolt could be realized for the required bandpass with the amplifier at 25°C. This is comparable to the signal for 0.5%  $O_2$  at STP. Reduction

of the bandpass after demodulation to 0.1 Hz (by integrating for 10 seconds) would further reduce the output noise by a factor of about 100. Increasing the amplifier temperature would increase the noise considerably, but satisfactory performance up to 125°C might be achievable provided the amplifier is located in the sensor, with no interconnecting cable noise.

In this connection, it is important to note that the performance and life expectancy of a preamplifier operating at 170°C are unknown, but it is almost certain that the sensor would not remain within specifications above 125°C, and it is probable that the amplifier would be permanently damaged within a short time if operated at 170°C. In this regard the RF sensor has a distinct advantage, in that it is possible to make a solid-state oscillator operate at 170°C.

#### 2.1.4.3 Alternatives Considered

Several alternative mechanical designs of the modified Greene-Hummel sensor are considered in the following paragraphs. The foregoing discussions of electronic noise and preamplifier bandwidth requirements also apply to these design alternatives.

### 2.2 Alternative Designs

#### 2.2.1 Evaluation of the Hornfeck Multiple Pole Approach

A sensor design utilizing multiple poles and pickup coils symmetrically arrayed about the axis of rotation of the chopper has mechanical design advantages compared to an asymmetrical sensor having one large pole and pickup coil. There may also be advantages with regard to adjusting the inductive noise component to optimum for the maximum chopper speed allowable mechanically.

A literature search conducted in the initial phases of the contract revealed U.S. Patent No. 2 467 211, issued to A.J. Hornfeck on April 12, 1949. This patent describes an oxygen sensor similar to Greene's except for the use of multiple poles symmetrically arrayed about the axis of chopper rotation (see Figure 5). This approach has mechanical design advantages, and also allows more freedom in the selection of design parameters for optimizing weight vs. sensitivity and for the control of the inductive noise component to maximize S/N at maximum allowable chopper speed. But it also has significant disadvantages.

##### 2.2.1.1 Disadvantages

The major disadvantage of utilizing multiple poles and coils lies in the geometrical relationship between the areas of each pole and the number of poles. The area per pole decreases approximately as the square of the number of the poles,  $n$ , when the desirable condition that there be four chopper segments between adjacent poles (each of the same area as the poles) is imposed. The signal decreases as the number of poles increases, but for the same total number of coil turns (divided between  $n$  small coils connected in series-aiding) the inductance decreases more rapidly. Consequently, for a given magnetomotive force and sensor size, the S/N (for the inductive noise component only) increases linearly with  $n$ . This permits more freedom for the optimization of total S/N at, say, a desirable maximum chopper speed. On the other hand, decreasing the signal by increasing  $n$  is feasible only to the limit set by the preamplifier voltage noise.

April 12, 1949.

A. J. HORNFECK  
METHOD OF AND APPARATUS FOR MAGNETICALLY  
DETERMINING GAS CONTENT

2,467,211

Filed Feb. 24, 1944

2 Sheets-Sheet 1

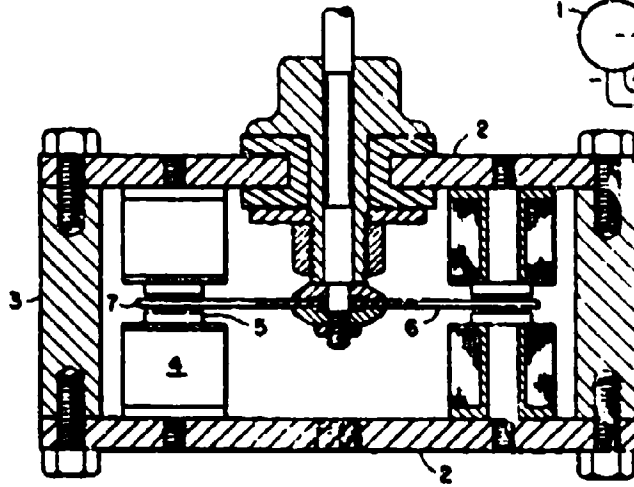


FIG. 2

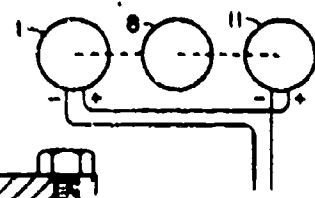


FIG. 6

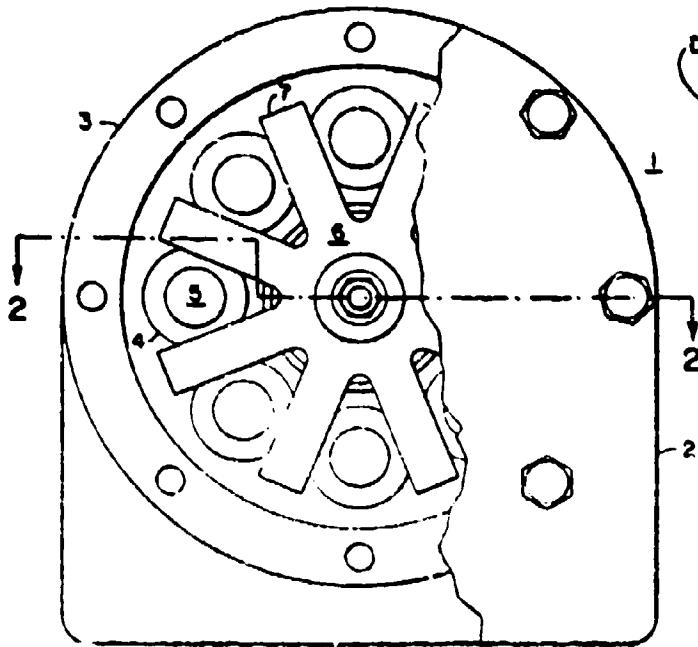


FIG. 7

FIG. 1

INVENTOR  
ANTHONY J. HORNFECK

BY *Raymond D. Jenkins*  
ATTORNEY

Figure 5. Hornfeck Multiple Pole Approach

### 2.2.1.2 Advantages

Using  $n$  small coils in series that have the same total number of turns as a single large coil requires a smaller mass of copper. The multiple pole approach, therefore, provides more freedom of choice in optimization of mass to sensitivity of the sensor. The coil total length also is less, making the coil resistance smaller for a given total number of turns and wire size. This factor makes it easier to make the Johnson noise and the resistive component of amplifier current noise negligible compared to the other noise source.

Better mechanical rigidity is one of the major structural advantages of the symmetrical multiple pole structure. The analytical study revealed that mechanical modulation of the pole gap is a noise source of concern. Specifically, the maximum random frequency modulation of the gap must be less than about one part in 100 million for the frequency spectrum covered by the preamplifier bandpass. Secondly, gap modulation at the chopper fundamental frequency must be stable to within about one part in one billion to cause less than a one-percent oxygen error (worst case). The study indicated that such mechanical stability should be feasible with materials with very high Young's modulus, such as the ferrites.

### 2.2.1.3 Alternative Multiple Pole Arrangement

In the event that a prototype sensor had shown excessive noise due to gap modulation and/or due to stray flux linkages with the magnetic structure, another multiple pole arrangement could have been employed to cancel such noise. In this configuration a double array of poles is employed. The two sets of poles and coils are located on two circles of different radius, both concentric with the chopper axis. The chopper is formed with zero-zero-zero-reference-zero-etc. sequence on one circle, and zero-sample-zero-zero-zero-sample, etc. sequence on the other. The two chopper and pole arrays are staggered in angle, so that when the coils are connected in series-opposing, the net signal is zero-reference-zero-sample. The "up-scale" reference chopper segment is more diamagnetic than the zero, so that when inverted by connecting those coils in opposition the net output reference appears as an up-scale (paramagnetic) signal. The smaller poles of the inner circle are fitted with coils of proportionately more turns to provide equal signals for equal modulation and stray flux linkages. Connection of the coils in series-opposing provides cancellation of all common-mode mechanical modulation and stray field effects. Since only one-half of the total coil is active at any time, the sensor S/N for electronic noise is reduced by a factor of two, all other conditions being equal.

### 2.2.2 Evaluation of the Rotating Magnetic Field Concept

A sensor design concept utilizing an outer flux path rotating around a stationary center magnet has the advantage of a large signal-to-weight ratio, but it is probably not feasible because it is not possible to have bearing tolerances that restrict the gap modulation to one part in one million.

Yet another mechanical design variation was considered briefly. In this version a hollow cylindrical magnetic structure is rotated about a fixed permanent magnet. The chopper consists of material in the cylindrical gap between the magnet and the cylindrical outer magnetic return path. The arrangement, illustrated in Figure 6, can be fairly long, increasing the pole area compared to that realizable with the thin chopper disc rotating in a plane discussed previously.

## BASIC FEATURES

FLOW-THROUGH SAMPLE CELL END-TO-END  
CENTER MAGNET STATIONARY  
OUTER FLUX PATH ROTATION  $\sim 3\ 600$  rpm  
SEALED ZERO AND REFERENCE CELLS (HOLLOW)

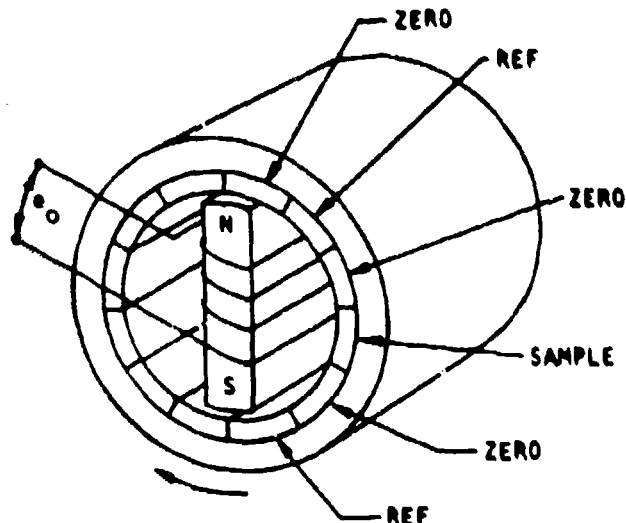


Figure 6. Rotating Magnetic Field  
Concept—End View

### The advantages are:

- Large pole area, providing large signal-to-weight ratio.
- Fabrication of hollow chopper reference segments is relatively simple, possibly making operation without thermal control feasible.

### The major disadvantages are:

- Rotation of the magnet and pickup coil is precluded by pickup coil slip-ring noise. Rotation of the outer structure is difficult.
- The impossibility of having bearing tolerances capable of restricting gap modulation to one part in one million is obvious. While the gap modulation of this structure would tend to be self-cancelling, it is not clear that such modulation would not make this design totally impossible.

### 2.2.3 Rationale for Selection of the RF Over the Greene-Hummel Approach

The analytical studies disclosed unexpected limitations of the Greene-Hummel approach which made it less attractive for further development than the RF

sensor. Furthermore, it was determined that the RF sensor performance could be considerably improved by using recent advances in electronics.

#### 2.2.3.1 Limitations of Greene-Hummel Approach

The analytical study of the Greene-Hummel sensor and the various modifications of it disclosed that major limitations were to be expected for a 5- (or even 15-) lb sensor. These limitations are summarized below, roughly in order of their fundamental impact on the development of a fuel-tank oxygen sensor:

- The signal will be about one millivolt per percent O<sub>2</sub> (STP).
- The S/N ratio for a solid-state, low-noise preamplifier at 25°C would be satisfactory, but it would be marginal at 125°C (or less), and the preamplifier would be either inoperative at 170°C or damaged by the exposure.
- Remote location of the preamplifier is not feasible because of cable noise, necessitating cooling to less than 125°C, which is not practical.
- The diamagnetic susceptibility of all solid chopper materials is so large that control of the sensor at maximum temperature (170°C) would be necessary.
- A vacuum tube preamplifier operating at 170°C might be feasible, but microphonic noise might then become the limiting factor.
- A complete prototype sensor would be required to verify the predicted performance, since none of the components could be tested without all of the others.

While these factors did not preclude the possibility of making a Greene-Hummel type sensor perform satisfactorily, they certainly reduced the probability of success within a reasonable development cost and ultimate production cost. Better approaches were sought, leading to the selection of the RF sensor.

#### 2.2.3.2 Advantages of the RF Sensor Approach

The basic RF sensor concept is not new, but all reported results showed that it fell short of meeting the required oxygen resolution by a factor of about 100, even under the best of laboratory conditions. For this reason it was not considered in the initial review of possible approaches. Later, however, in the analytical study of the capabilities of this approach, the latest advances in the state of the art of electronics were applied. It was concluded that with modern techniques and components the RF approach was preferable to the Greene-Hummel (see Table V). The Major advantages compared to the Greene-Hummel approach are:

- Signal level in the several-volt range, with measurement determined by the period of a beat frequency.
- A solid-state oscillator operating at 170°C is feasible, while a low-noise, solid-state amplifier is not feasible.
- Temperature control is mandatory for the RF sensor, but the study indicated that it would also be required for the Greene-Hummel sensor.

Table V. Summary of Advantages of RF Approach  
over Greene-Hummel Approach

<u>Factor Compared</u>	<u>RF Compared to Greene-Hummel</u>
● Signal Level	- much better
● Complexity of electronics	- less complex
● Reliability of electronics	- better
● Thermal errors	- better control required
● Pressure errors	- same
● Critical tolerances	- much less critical
● Ultimate weight	- considerably less
● Ultimate power	- probably less
● Ultimate cost (production model)	- considerably less

- Feasibility of each major component of the RF sensor could be demonstrated independently, reducing the risk of development funds involved in the other approach.
- The RF sensor components are inherently of lower mass.
- The precision required for mechanical components is inherently less severe.
- The ultimate cost of production model sensors should be less than for the Greene-Hummel sensor.

A decision was made to pursue the RF approach only, since funding did not permit parallel efforts. Section 3 describes the RF sensor in greater detail.

### 3.0 SYSTEM DESCRIPTION

#### 3.1 Overall System Description

The system is basically very simple. The essence of the oxygen measurement is a change in frequency of a radio-frequency (RF) oscillator due to the paramagnetism of oxygen.

The main elements of the RF oxygen sensor are a sampling chamber, a radio-frequency oscillator, a zero reference "chopper," a reference crystal oscillator, and a chopper actuator. The inductor (sensing coil) of the RF oscillator is enclosed in the sampling chamber. The frequency of oscillation shifts in direct proportion to the partial pressure of oxygen due to the effect of its unique paramagnetic property on the flux field of the inductor. The change in the RF oscillator results in a difference frequency. This is digitized and fed into a binary up-down counter. During a 13-second interval, eight "up" counting periods occur with the chopper in the sampling chamber and eight "down" counting periods with the sample gas in the chamber. At the end of the 13-second period, the data on

the oxygen concentration are converted to an analog output for recording and/or direct meter readout. It should be noted that the specification allows a 30-second readout period. Our output would be more accurate if the data were averaged over this period of time. However, our analyses indicated that system accuracy would be adequate even though a 13-second period is used.

The sampling chamber and sensing coil, along with the oscillator electronics, are designed to operate in a thermally controlled zone. This zone would be held at  $170 \pm 1^\circ\text{C}$ . The laboratory breadboard model developed used a manually tuned frequency synthesizer, Hewlett-Packard Model No. 3100A, in place of a crystal oscillator. A flight unit would use a crystal oscillator with a phase-locked loop.

The RF sensor approach provides a theoretical resolution of about 0.04%  $\text{O}_2$  at sea level. At altitudes or pressures differing from one atmosphere, an absolute pressure measurement is necessary to be able to convert the oxygen partial pressure measurement to percent oxygen by volume. This was not implemented in the breadboard model.

The system was breadboarded in two mechanical configurations, MOD I and MOD II (see Figures 7 and 8). As a result of testing the first MOD I configuration, it was evident that to achieve the desired resolution and accuracy the system would have to be designed and assembled to be insensitive to mechanical vibrations that are synchronous to the chopping frequencies. The MOD II configuration included design changes to provide the mechanical stability that was determined to be needed for successful operation (see Subsection 4.2.1). Details of the two mechanical designs and the electronics are presented in the following paragraphs.

### 3.2 Electronics

#### 3.2.1 Overall Electronics Design

Except for the signal measurement and conditioning circuits, all circuits and components are standard off-the-shelf items or of common design.

The overall electronics associated with the signal measurement and conditioning is shown in the block diagram in Figure 9. The oscillator circuit is the only portion of the electronics that would need to be exposed to the fuel-tank environment. It is shown attached to the outer shield in the photos of Figures 7 and 8. The rest of the electronics fabricated for the breadboard are housed in the separate chassis shown in Figures 10, 11, and 12.

Supporting electronic circuits used in operating the breadboard include a stepper motor and ramping driver, motor position sensor and control, and temperature controller. These are off the shelf or of common design and discussion of them does not contribute to the explanation of the measuring system.

#### 3.2.2 Functional Description of the Measurement Oscillator

The critical part of the electronics is the measurement oscillator, since a difference in oscillator frequencies between when the sensing coil is surrounded by an air mixture and when it is surrounded by a zero reference is the basis for the oxygen measurement. The required oscillator stability is

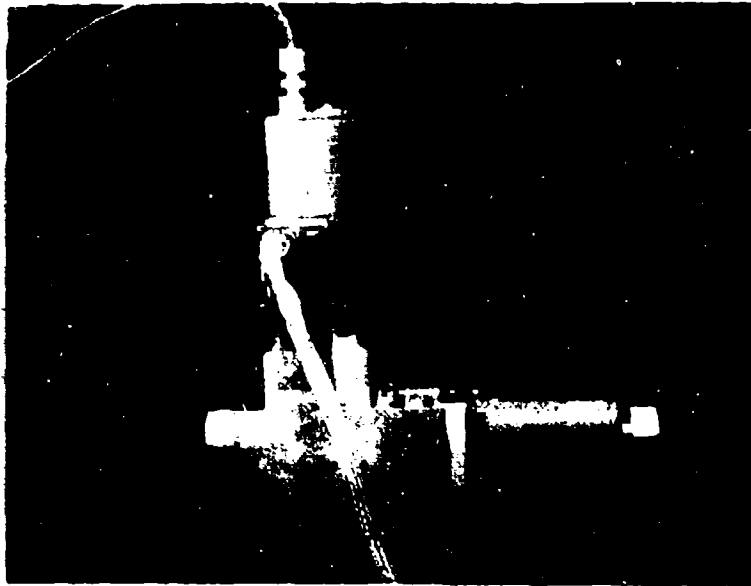


Figure 7. Configuration of MOD I Laboratory Breadboard Model

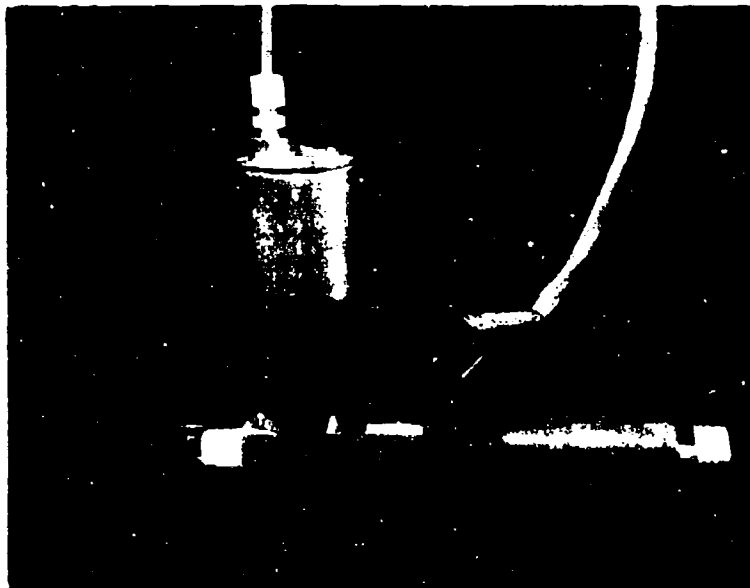


Figure 8. Configuration of MOD II Laboratory Breadboard Model

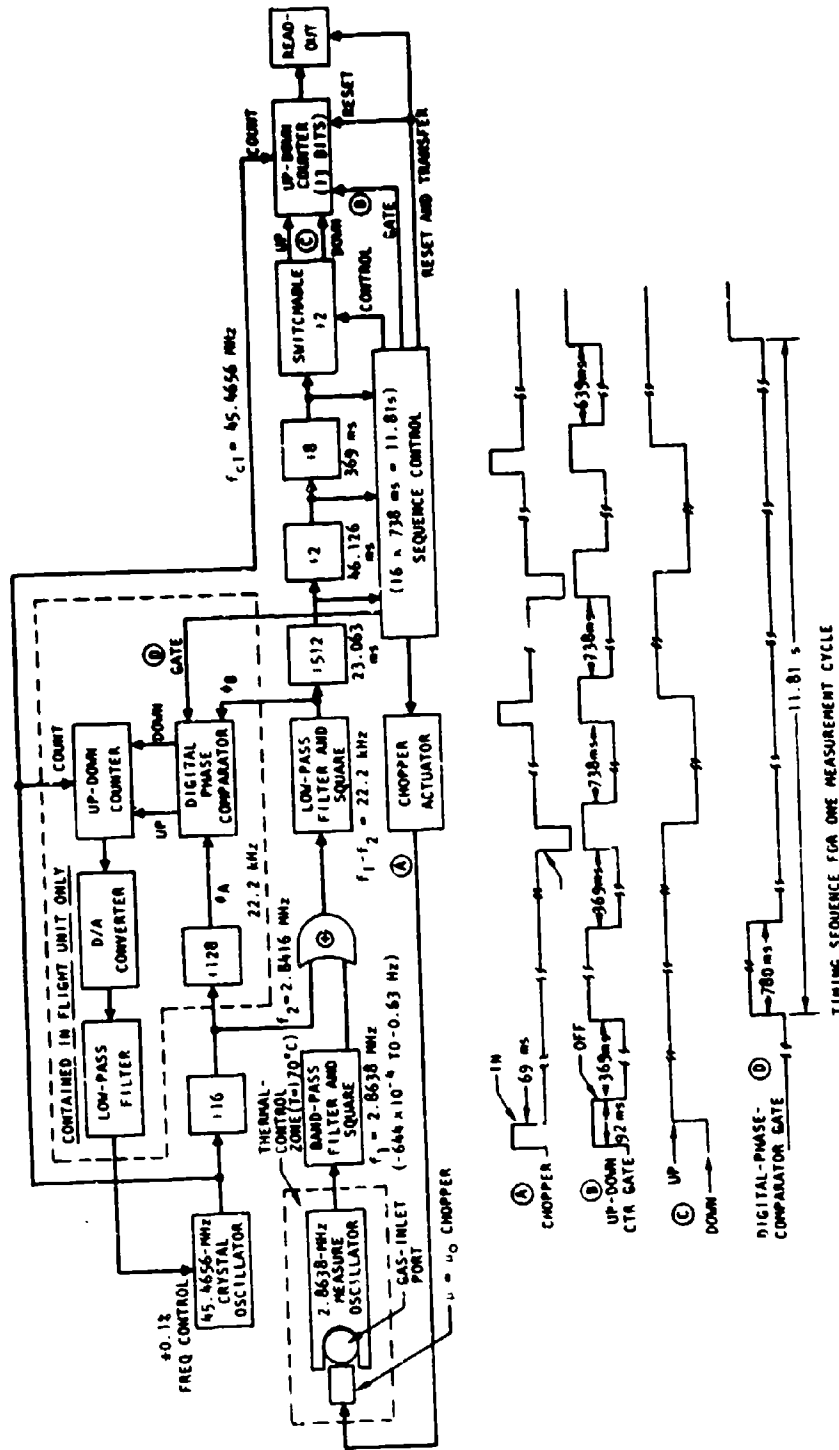


Figure 9. Overall Electronic Design of Oxygen Fuel-Tank Sensor

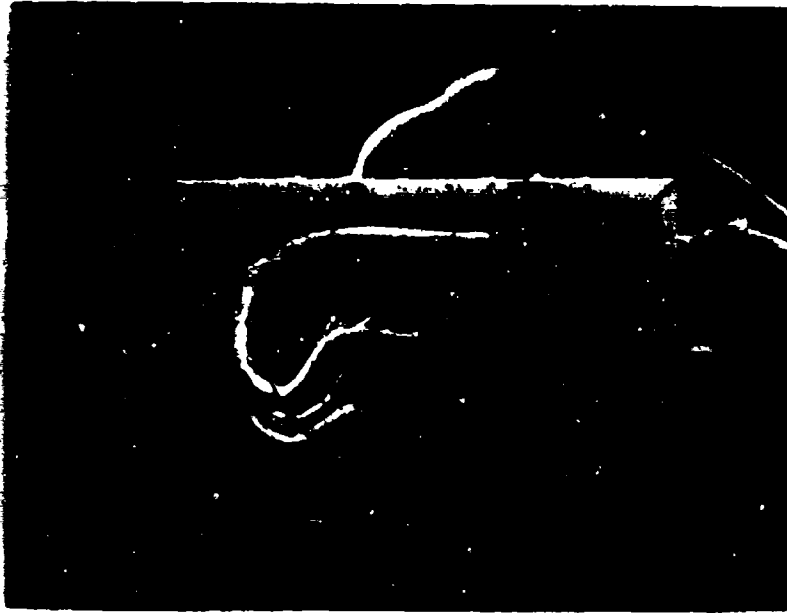


Figure 10. Bandpass Filter

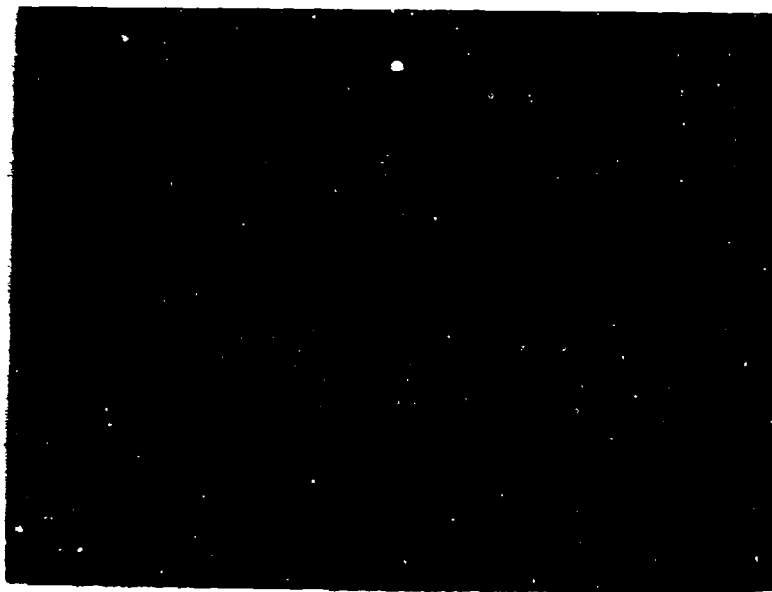


Figure 11. Digital Electronics

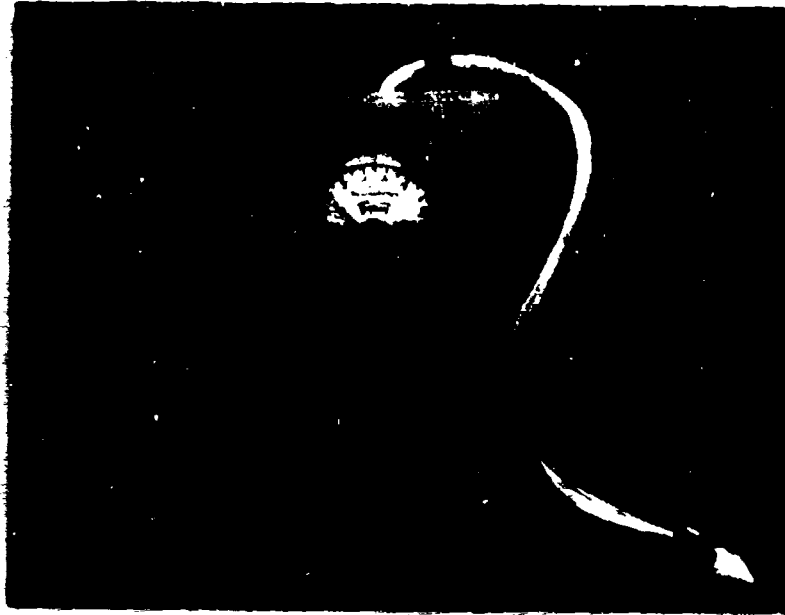


Figure 12. Digital-to-Analog Converter

met by the inherent design of the oscillator, by the fact that stability is required for only 738 ms, and by the addition of a phase-locked loop that tunes the crystal oscillator to maintain the required 22.2 kHz beat frequency.

The heart of the system is the measurement oscillator. The schematic for this circuit is shown in Figure 13.

### 3.2.2.1 Coil Q Requirement for Optimum Signal

The inductor, L1, of the tank circuit is the "sensing" coil. This inductor is formed of 5 turns of Litz wire approximately 1 in. in diameter and 3/8 in. long. The Litz wire is made of 104 braided strands of 44-gage wire with varnish insulation and a cotton cover. This permits operation to 125°C.

The Q of the coil should be 200 for obtaining an optimum signal. We have achieved a Q of 92 in the breadboard. This might be improved with an optimum Litz wire of a larger number of strands of smaller diameter, e.g., 450 strands of 60-gage wire. This was not available off the shelf, although similar wires have been made.

### 3.2.2.2 Basis for the Oxygen Measurement

The difference in the oscillator frequency when the sensing coil is surrounded by an air mixture compared to that when the coil is surrounded by the zero reference chopper is the basis for the oxygen measurement. The nominal oscillator frequency is 2.8638 MHz. The frequency change between the zero reference and 21% atmospheric oxygen is approximately 1/2 Hz. Obviously oscillator stability is a major requirement. The required stability during the measurement period is indicated in the following calculations.

### 3.2.2.3 Calculation of the Required Oscillator Stability

From the literature, the volume susceptibility of 100% oxygen at 0°C and one atmosphere is  $1.95 \times 10^{-6}$ . Assuming the chopper is zero, the change in volume susceptibility is

$$4\pi K = 1.95 \times 10^{-6}$$

At 170°C, the operating temperature of the sensor

$$4\pi K = 1.95 \times 10^{-6} \left( \frac{273}{443} \right)^2 = 0.74 \times 10^{-6}$$

For 2 psia pressure at this temperature

$$4\pi K = 0.74 \times 10^{-6} \times \frac{2}{14.7} = 0.10 \times 10^{-6}$$

for 0.1% resolution,

$$4\pi K = 0.10 \times 10^{-9}$$

This implies an oscillator stability of

$$\frac{1}{0.10 \times 10^{-9}} = 1 \text{ part in } 10^{10}$$



However, a novel feature of this approach is that this stability is only required during the sampling interval of 738 ms. Tests have shown the breadboard oscillator to remain stable to 0.01 ppm for one hour or more,

#### 3.2.2.4 Need for Phase Locking

In the breadboard, the clock frequency must be manually retuned to maintain the 22.2 kHz difference frequency. If the measure oscillator drifts, the amplitude of the signal from the low-pass filter will drop and noise will increase. Within the limits of the filter bandwidth, slight changes are cancelled out by the up-down counting logic. To permit long-term operation, a phase-locked loop must be added. This will monitor the 22.2-kHz signal and correct it to maintain that frequency by varying the bias to an E-CAP that will modulate the 45-MHz crystal clock. That is, during the zero-reference interval, the difference frequency is varied to bring the difference frequency back to 22.2 kHz. In the breadboard, the 45 MHz is supplied by a manually tuned frequency synthesizer, Hewlett-Packard Model No. 5100A.

#### 3.2.3 Calculation of System Resolution

The system resolution can theoretically meet the 0.1-percent specification requirement. The following calculations determine the system resolution:

The number of counts in the binary output is given by

$$N = \frac{d\mu}{\mu} \left( \frac{f_1}{f_1 - f_2} \right) \frac{f_{cl} \cdot T_o}{4}$$

where

$$\frac{d\mu}{\mu} = 1.007 \times 10^{-9} \left( \frac{P_T}{2 \text{ psia}} \right) \left( \frac{n_{O_2}}{1\%} \right)$$

$$\begin{aligned} \frac{f_{cl} \cdot T_o}{4} &= 45.4656 \times 10^6 \times \frac{11.81}{4} \\ &= 1.34 \times 10^8 \end{aligned}$$

$$\frac{f_1}{f_1 - f_2} = \frac{2.8638 \times 10^3}{22.2} = 129$$

Thus

$$N_{170} = 17.4 \left( \frac{P_T}{2 \text{ psia}} \right) \left( \frac{n_{O_2}}{1\%} \right)$$

The counting resolution per counting period is estimated to be 0.41 counts per measurement. Since there are 8 measurements per 12 seconds, the rms error will be

$$0.41 \sqrt{8} = 1.16 \text{ counts rms/12 s}$$

Thus, the output resolution will be

$$\frac{1.16}{17.4} = 0.07\% \text{ O}_2 \text{ at 2 psia and } 170^\circ\text{C}$$

The maximum number of counts accumulated during a 12-second period at 170°C can be estimated as

$$N_{\text{max}} = 17.4 \left( \frac{25 \text{ psia}}{2 \text{ psia}} \right) \left( \frac{15\% \text{ O}_2}{1\% \text{ O}_2} \right) = 3262$$

This would require a 12-bit counter. However, the output during ambient laboratory tests would be

$$N_{25} = \left( \frac{14.7}{14.7} \right) \left( \frac{21}{1} \right) = 5935, \text{ requiring a 13-bit counter.}$$

The breadboard has a 14-bit counter to permit testing with higher oxygen concentrations.

The output of the binary counter is put through a digital-to-analog converter to permit continuous recording of the output. This analog output could be supplied to a meter to provide a direct reading of percent oxygen concentration. However, if the meter were scaled for sea level, then to operate at pressures other than sea level, a pressure correction would have to be made to convert the partial pressure measurement of oxygen to a volume percentage reading. A pressure transducer was not incorporated into the breadboard.

### 3.3 Mechanical

#### 3.3.1 Details of the Mechanical Design

The mechanical design must contain the flux surrounding the sensing coil and alternately expose the flux field to sample gas and a zero reference chopper. The chopper actuation must be precisely timed and must not mechanically disturb the system even to the extent of a fraction of a microinch.

##### 3.3.1.1 Impact of MOD I Tests

The MOD I tests indicated the criticality of relative movements between parts associated with the sampling volume. It also showed that vibrations imparted to the oscillator electronics were a noise source. The magnitude of the noise level and drift rate was excessive. However, as the tests did indicate that oxygen measurements were being achieved, it was decided to redesign the assembly and eliminate the identified noise sources. To accomplish this, a completely new mechanical assembly was made. The layout of MOD II is shown in Figure 14. The photograph, Figure 15, shows the major parts.

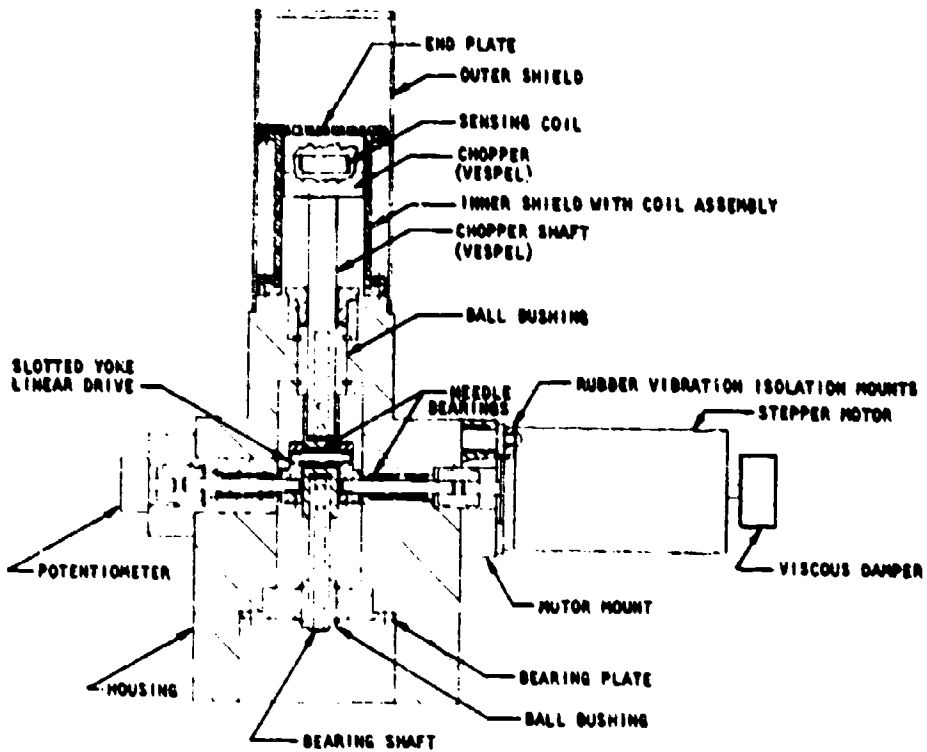


Figure 14. Mechanical Configuration of Aircraft Fuel Tank O<sub>2</sub> Sensor



Figure 15. MOD II--Internal Parts

### 3.3.1.2 MOD II Chopper Design

The chopper in this assembly is actuated through a slotted-yoke linear drive. The chopper shaft is positioned by two linear ball bushings. These bushings absorb the slight couple introduced into the chopper shaft by the slotted-yoke drive. Very close axial alignment is thus maintained so the chopper can move without touching the inner shield or the sensing coil mount. Chopper clearances are held to .010 inch to "chop" as large a sampling volume as possible.

### 3.3.1.3 Flux Field Containment

The flux field containment was improved by closely fitting the lower shield around the Vespel shaft. The upper and lower plates are now 1/8-in. copper plate, where previously a screen was used. The sensing coil mount is now clamped by an interference fit under the upper end plate. The three radial arms of the coil mount were previously simply held by friction in slots in the inner shield.

### 3.3.1.4 Coil Mount and Chopper Material

Both the coil mount and chopper are made of Vespel instead of Teflon. The Vespel is dimensionally stable, is much harder, is machinable to close tolerances, and has acceptable electrical properties. It is also resistant to hydrocarbons in jet fuel.

### 3.3.1.5 Stepper Motor

The MOD I stepper motor was retained as the actuator, as all the drive electronics were available and positioning accuracy with this method has been proven. The stepper motor inherently generates vibrations and ultimately should be replaced as the prime mover. A viscous damper and rubber mount were used to minimize vibration transmission to the chopper housing.

The bulk and weight of the breadboard model would be reduced considerably in a flight configuration model.

## 4.0 TEST RESULTS

### 4.1 Static Tests

#### 4.1.1 Testing to Determine How to Achieve Maximum Inductance

Tests of different gap areas as well as the effects of shielding, different ferrite materials for the inductor core, and different coil configurations of an air core inductor were made to determine the maximum inductance that could be acted on by the paramagnetism of oxygen to result in the largest frequency change of the sensing oscillator. Based on these results and available material, we evolved an air core inductor coil of 1 in. OD by 3/8 in. long, with a Q of 92.

As part of the development effort, tests were conducted on subassemblies to optimize the design. These tests are designated "static" tests to differentiate them from the operational system tests.

A major problem in the development of this system was associated with the sensing oscillator. There was difficulty in determining how to achieve the

maximum inductance that could be acted on by the paramagnetism of oxygen to result in the largest possible frequency change of the sensing oscillator.

The inductor was first configured as a toroid made of ferrite. For this configuration a 1/2-cm gap with a 1-cm<sup>2</sup> gap area would be chopped by a beryllium oxide zero reference. This gap should control 90% of the inductance, giving the desired frequency change. Calculations indicated a Q of 200 was possible with a 0.6  $\mu$ H inductor. However, when tested, the inductance was low by a factor of eight. It was concluded that this was due to flux leakage fields. Consequently, the ratio of the gap area to gap length was increased and electrostatic shielding was added to prevent the stray fields. While improvements resulted, only about 50% of the inductance was controlled by the gap, and Qs less than 100 were obtained.

Various other ferrite compositions were examined and also other inductor configurations. A gapped cup design was also tested. Instead of flat pole faces, two cups--each about 1/2 in. in diameter and containing a central rod--were positioned with the opposing faces 1/8 inch apart. Again, results were improved but not enough to provide adequate signal.

An air-core coil was the final alternative. Here control of the flux was simplified since it could be contained in an electrostatic shield. The main problems were then to maximize the Q and determine how the chopping action could be implemented. Instead of simply chopping a gap, the coil had to be surrounded so all the volume within the electrostatic shield could be filled alternately with sample gas and zero-reference material. An inductor 1-3/8 in. OD by 5/8 in. long was made of solid 10-gage wire. This required an electrostatic shield 4 in. ID by 3-1/2 in. long, which would have required a chopper the size of an automotive engine piston. Tests using different sample gases, without a chopper, proved that oxygen did cause a shift in the oscillator frequency in close agreement with the calculated value.

Effort was then directed at reducing the coil size so a minimum sample volume could be obtained that would be possible to chop. As we were operating on a frequency range of 2.5 MHz, conductivity was confined to the surface and, therefore, the larger the surface area, the smaller the inductor could be made. Calculations showed that multistranded Litz wire would be an advantage. A 183-strand, 44-gage wire could be made into a coil 3/4 in. OD by 1/4 in. long. A 413-strand inductor might be as small as 3/8 in. OD by 1/3 in. long. Such wires have been made commercially, but because we were limited by off-the-shelf availability, we could not optimize coil size and therefore used a 104-strand, 44-gage construction for the MOD I and MOD II tests. This resulted in a coil 1 in. OD by 3/8 in. long, with a Q of 92.

#### 4.1.2 Testing the Chopper to Determine Positioning and Timing Accuracy

Tests were conducted to determine the chopper allowable drive pulse rate, positioning accuracy, and residual vibration. As a result, the time allowed to move the chopper from one position to another was increased from 23 to 69 ms and settling time was increased from 23 to 46 ms.

A second major problem was in actuating the chopper to move it in and out of the sampling volume within the required time intervals and with precise

positioning. It was decided to use a stepper motor to do this. A Slosyn Model M063-FD09 was selected. It is designed to rotate 1.8 degrees for every timing pulse applied to its field coils.

To move the chopper in or out requires 180 degrees of rotation or 100 pulses. Since the movement must be accomplished in 69 ms, the average pulse rate must be 1 430 per second. The motor can respond to 10 000 pulses/s but cannot start or stop at that rate without slewing or missing some pulses. As we must maintain precise synchronization, no slippage is allowable. It was therefore necessary to design a pulse generator that would apply pulses at a low starting and stopping rate. A pulse train, starting at 500 pulses/s, ramping to 1 600 and then returning to 500, was designed. A 5-k $\Omega$  potentiometer was attached to the motor shaft to check its position and motor response.

Tests were then made to determine the allowable drive pulse rate, positioning accuracy, and residual vibration. The tests consisted of allowing the motor to move the chopper in and out 100 times while monitoring the resistance of the readout potentiometer. This was done at nominal stepping rates of 1 540 pulses/s for the high-speed portion of the motion, and repeated at 1 925 and 2 220 pulses/s. At 1 540 and 1 925 pulses/s, operation was correct, while it was erratic at 2 220 pulses/s. This means that the 69-ms period is adequate for the chopper movement but cannot be reduced to 23 ms, which was the original time used in designing the logic.

A measurement was made to observe the braking characteristics of the motor by applying 5 V to the readout pot and observing the waveform on a scope. We observed a 14-degree peak-to-peak, 4-ms period oscillation which decayed sinusoidally as the motor came to rest. The ringing was still noticeable 30 ms after the end of the pulses. The logic allowed for a 23-ms settling period before sampling data was taken. The logic was revised to allow 46 ms to assure that the chopper had come to a complete stop.

#### 4.2 Functional Tests (MOD I)

##### 4.2.1 Test Results for the MOD I Configuration

The MOD I testing validated the basic measurement concept and led to an understanding of the sources of drift and noise.

Tests were conducted on two different system configurations. The first configuration, MOD I, served to prove that the basic measurement concept was valid; that is, that low concentrations of oxygen could be detected in the presence of nitrogen, carbon dioxide, and fuel vapors. However, the MOD I configuration also revealed technical problems that would have to be overcome to achieve the accuracy, resolution, and stability required for a practical instrument. Proof that these problems are solvable with continued development is evident from the improved performance of the MOD II configuration.

Measurements were made on the MOD I system with nitrogen, 5 and 10% oxygen in nitrogen, 10% carbon dioxide in nitrogen, air (21% O<sub>2</sub>), and propane. The results of these tests are shown in the strip chart recording of Figure 16. It is apparent that the response is repeatable with the different test gases. Carbon dioxide and nitrogen have substantially an identical response. The response to an increasing oxygen concentration appears to be linear, which is as it should be.

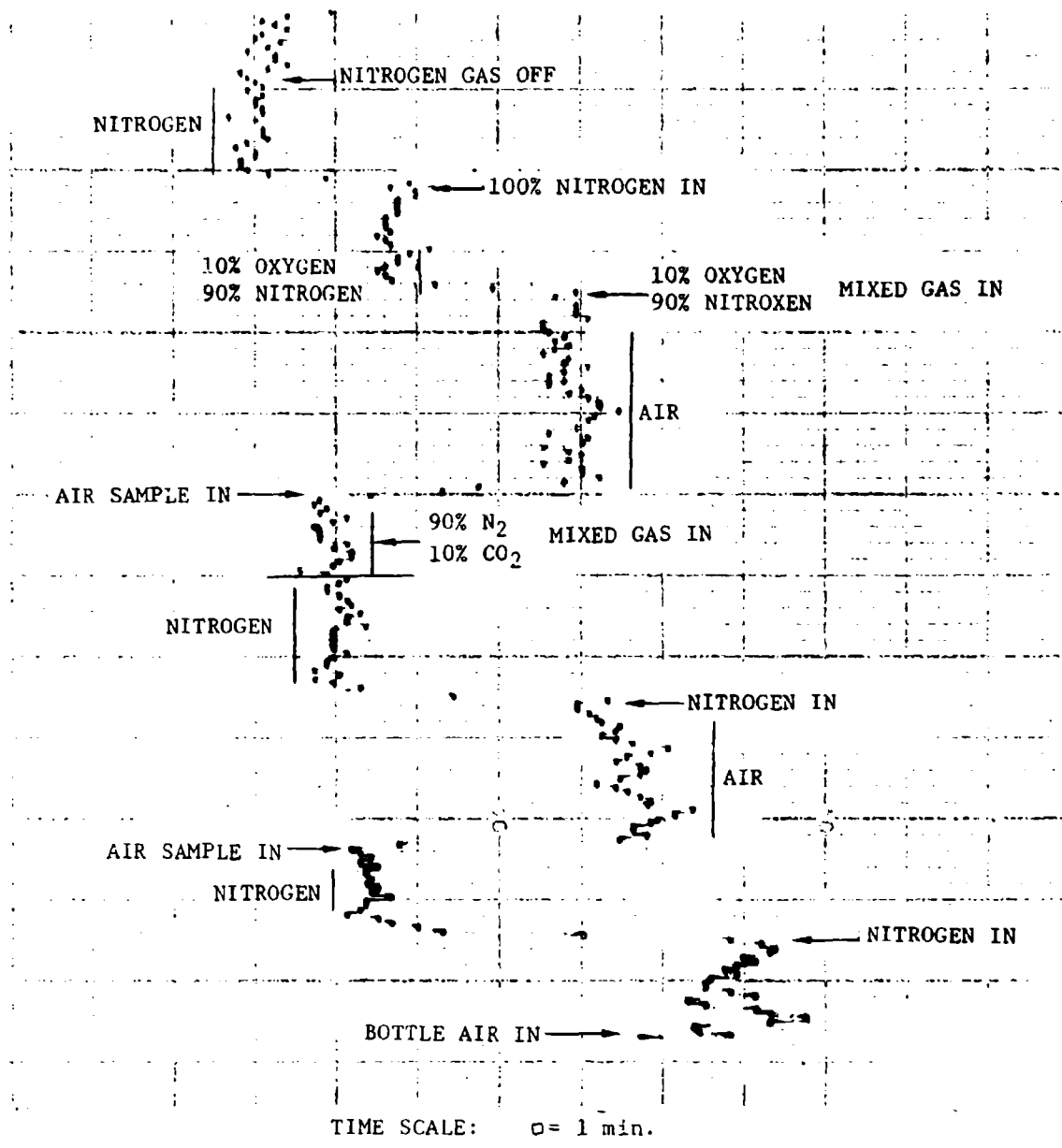


Figure 16. MOD I--Sample Gas Tests

The results of the MOD I test are not precise because of a noise level of approximately  $\pm 3\%$  oxygen plus drifting. The drifting was not caused by temperature changes, since the temperature was monitored and was never changed more than  $1^\circ\text{C}$  during the test. Changes up to  $1^\circ\text{C}$  per 100 seconds should not affect the output.

To determine drift and noise level, the system was operated continuously for a period of seven days. During this time it was simply exposed to ambient air. The output was recorded on a strip chart. At the end of the seven-day period, the chopper was stopped and the electronic noise level determined. This showed that the system was capable of operating continuously. The output tended to drift slowly with a random pattern. The noise level increased several fold periodically and then returned to its normal level without adjustments.

As a result of these tests, we gained considerable insight into the sources of the noise and the drifting, which are discussed in the following paragraphs.

#### 4.2.2 Noise Sources Related to Output Counts and Frequency Changes

Before examining the sources of the noise and drift, we summarize the general scale of effects leading to the oxygen measurements. Output counts and frequency changes are the two parameters of interest.

At  $170^\circ\text{C}$  and for the chopper operating on all of the volume in which the magnetic field from the sense coil lies, the following equation relates the output number of counts,  $N_{170}$ , to the oxygen concentration,  $\eta_{\text{O}_2}$ , at a total pressure,  $P_T$ :

$$N_{170} = 17.4 * \left( \frac{P_T}{2 \text{ psia}} \right) \left( \frac{\eta_{\text{O}_2}}{1\%} \right). \quad (1)$$

Because of the  $T^{-2}$  dependence of paramagnetism in a gas, this equation becomes at  $25^\circ\text{C}$

$$N_{25} = 38.5 * \left( \frac{P_T}{2 \text{ psia}} \right) \left( \frac{\eta_{\text{O}_2}}{1\%} \right) \quad (2)$$

or referred to one atmosphere pressure

$$N_{25} = 283 * \left( \frac{P_T}{1 \text{ atm}} \right) \left( \frac{\eta_{\text{O}_2}}{1\%} \right). \quad (3)$$

---

\*The calculation of these constants is provided in Section 3.0, System Description

Under laboratory conditions where  $P_T = 1 \text{ atm}$  and  $n_{O_2} = 21\%$ , then

$$N_{\text{atm}} = 5\,935 \text{ counts} \quad (4)$$

This number is 5 to 10% high because the chopper fills only 90 to 95% of the field volume.

The outputs given by equations (1) through (4) reflect frequency changes given by

$$\left. \frac{\Delta f}{f} \right|_{170} = 5.3 \times 10^{-10} \left( \frac{P_T}{2 \text{ psia}} \right) \left( \frac{n_{O_2}}{1\%} \right) \quad (5)$$

at  $170^\circ\text{C}$ , and at  $25^\circ\text{C}$  by

$$\left. \frac{\Delta f}{f} \right|_{25} = 8.6 \times 10^{-9} \left( \frac{P_T}{1 \text{ atm}} \right) \left( \frac{n_{O_2}}{1\%} \right), \quad (6)$$

$$\text{in that } \Delta N = 3.43 \times 10^{10} \left( \frac{\Delta f}{f} \right). \quad (7)$$

$$\text{or } \Delta N = 1.2 \times 10^4 (\Delta f_{\text{Hz}}). \quad (8)$$

#### 4.2.3 Measurement of Electronic Noise with Chopper not Moving

##### 4.2.3.1 Pulse-Height Analyzer Measurement

Using a pulse-height analyzer, the measured rms electronic noise at room temperature when the chopper was not moving was 8.5 counts. This corresponds to 0.49% oxygen at  $170^\circ\text{C}$  and a total pressure of 2 psia, or to 0.035% oxygen at  $25^\circ\text{C}$  and 1 atmosphere. This noise level resulted from rms frequency shifts of  $2.5 \times 10^{-10}$  parts in 2.86 MHz or  $7.15 \times 10^{-4}$  Hz. Clearly, if this variation had been the only noise source, then we should have achieved a nearly noise-free measurement of the 21% oxygen in the earth's atmosphere at sea level.

##### 4.2.3.2 Strip Chart Recorder Measurement

When the electronic noise (chopper not moving) was recorded on a strip chart (Figure 17), however, it was approximately equivalent to 1-1/2% oxygen. The apparent increase in noise when measured on a strip chart as compared to the pulse-height analyzer was due to the manner in which the bits from the binary counter were transferred through the digital-to-analog converter. Also, the theoretical output is 50 chart divisions for 21% oxygen, or 2.38 divisions per 1% oxygen. However, we only saw a change of about 0.84 divisions per 1% increase in oxygen. Since the electronic noise is independent of chopper operation, the oxygen equivalent is  $1.5 \div 2.38$ , or 0.63%. This is about 178 counts.

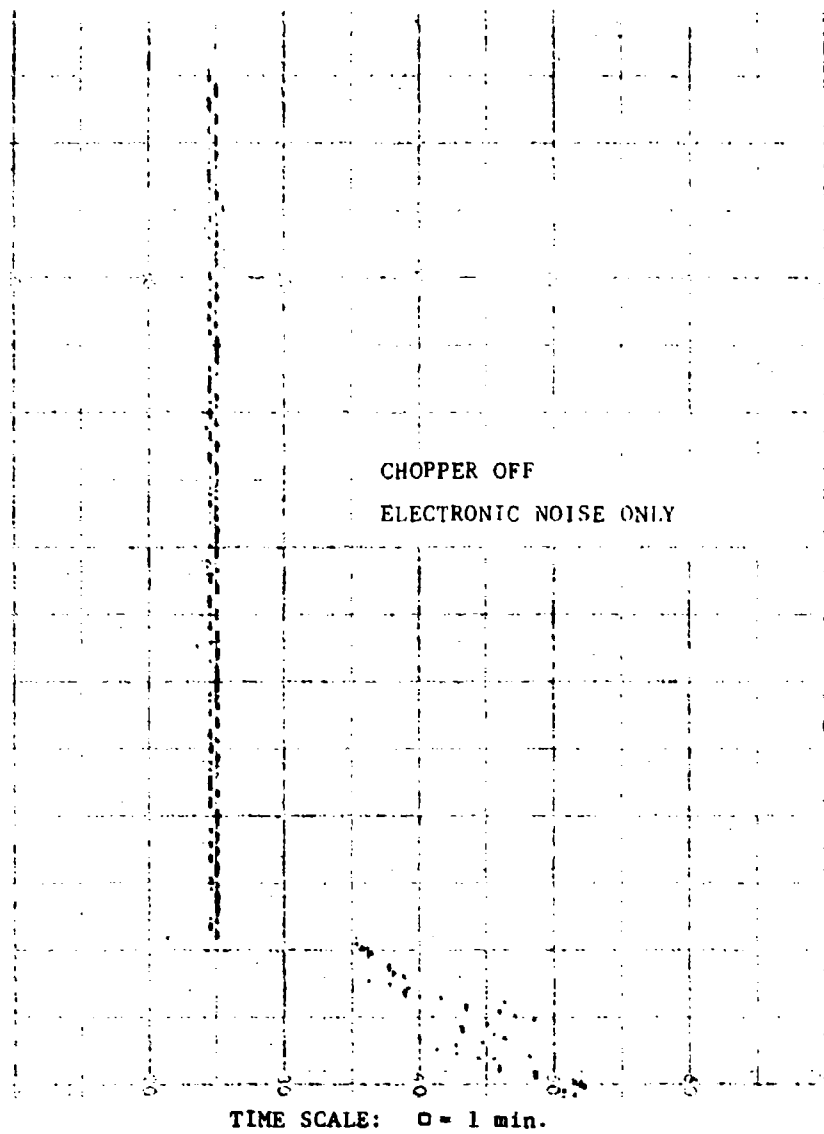


Figure 17. MOD I--Electronic Noise Only (Chopper Off)

Chopper operation produced both baseline drifts and an increased noise level. After analytical and experimental investigations, the most probable cause appeared to be mechanical instabilities involving the magnetic field from the sense coil.

When the chopper was operated, two degrading effects appeared. First, monotonic drifts with instantaneous rates near 600 counts/min. lasted for periods of several minutes, producing baseline changes up to 16 000 counts in about 1/2 hour. This drift did not always have a constant rate but did appear to maintain the same sign for times approaching one hour, although it sometimes flattened out or reversed in longer periods. Second, the random scatter about a line of constant drift was about 100 counts, rms, in comparison to 8.5 counts for the still chopper. Results this good were only achieved after securing the oscillator to the chopper barrel, inserting a flexible coupling in the motor shaft, isolating the motor from the chopper itself, and tightening both the upper and lower screens as much as possible. The chopper was initially synchronized manually, and no mechanical stops were present for further synchronization. An optical synchronizer was available but was not used because of instabilities caused by the temporary flexible coupling in the motor shaft.

Diamagnetic Effects of Teflon Chopper--We investigated various causes of these drifts both analytically and experimentally. For example, using an 8-digit counter we measured the diamagnetic effect of the Teflon chopper body after eliminating its dielectric effects with a high-resistivity Aquadag (graphite) coating. The frequency shift caused by the Teflon was about 20 Hz, corresponding to 240 000 counts at the output (see equation (8)). We can explain this frequency shift by a mass susceptibility of  $0.4 \times 10^{-6}$ , which is a value typical for organic compounds.

In order to obtain shifts near 16 000 counts, we had to assume that the effect of Teflon changed 6.7% in about 1/2 hour. However, temperature was not likely to cause such changes because the diamagnetism of a solid depends only to a small extent on temperature at a rate near 10 ppm/°C. Thus a 6.7% change would have required an impossible temperature transient.

Furthermore, the positioning accuracy of the plunger at the ends of its travel was not likely to have caused these shifts. Because the crankshaft wrist-pin design for the chopper drive produces a quadratic (cosine) dependence for the motion of the chopper near the limits of its travel, small angular displacements of the motor shaft would produce even smaller changes in the chopper position when it stops. For example, if the chopper travels 1 in. for 180 shaft degrees, then a 1.8-degree shaft error, corresponding to one step of the motor, would produce only a 0.25-mil error in the rest position of the chopper. Thus, if the Teflon diamagnetic offset of 240 000 counts had been linearly related to the chopper motion, this rather large angular error would have translated into 60 counts. However, the magnetic field from the coil was concentrated near the coil itself and not near the boundaries of the Teflon chopper at rest, making the output dependence on the chopper position less than linear and indicating that about 3 counts was a reasonable estimate for the effect of a 1.8-degree shaft error. Thus, we do not consider the diamagnetic offset from the Teflon

chopper to have been a likely cause of the 16 000 count drifts. Dielectric effects after the Aquadag shielding were probably smaller than the diamagnetic effects and thus could also be eliminated.

Effects of Thermal Transients--We also considered thermal transients causing errors as a result of the 10 ppm/°C temperature coefficient of the oscillator. Assuming a large temperature change of 10°C applied with a 1000-s time constant to produce a change lasting over 16 minutes, then the largest effect on the output would be 0.5 counts, neglecting the effects of the nonzero dead time during the chopper motion. This thermal transient would have caused frequency drift rates of 3 Hz/10 s, which were in fact occasionally present during tests with the static chopper. Under those conditions, including the delay for chopper motion, noise levels were small compared to 100 counts and no offset effects approaching 16 000 counts in the baseline were ever observed. Thus, the temperature coefficient of the oscillator is not likely to have been the source of these drifts.

Conclusion--We were thus led to the conclusion that various mechanical instabilities directly involving the magnetic field from the sense coil were the most likely source of the baseline drifts and increased noise level. In order to obtain a baseline drift in distinction to random noise, the coil inductance would have to vary relatively rapidly in synchronism with the chopper, and then the amount of this modulation would have to change slowly over time periods approaching one hour. In order to obtain a 16 000-count baseline drift, equation (7) indicates that the modulation in frequency would have to be at least 0.5 ppm, corresponding to an inductance modulation of 1 ppm. We investigated several sources of modulation of this magnitude, which are discussed in the following paragraphs.

#### 4.2.5 Effects of Screen and Metallic Crankshaft Modulations on Baseline Drift and Noise Level

Both screen motion and the metallic crankshaft were secondary contributors to the noise and baseline drift. Screen noise was considerably reduced by adding stiffening; and it was expected that improving the shielding between the crank and the coil, securing the shielding better, and properly synchronizing the chopper motor would reduce the effects of the metallic crankshaft.

Screen Motion--It was realized that the noise level was extremely sensitive to the rigidity of the mounting of the upper and lower screens. The addition of stiffening members to the screens was necessary to obtain any consistent data on a scale of 16 000 counts. This fact was not surprising in that the screens determined about 2% of the inductance, and thus motions of 50 microinches could cause sudden 16 000-count steps. This problem was compounded by the gas-derived pulsations applied to the screens by the chopper motion and the insecure nature of the set-screw fastening for the upper screen. The set screws were a particular problem in that if they were set tight enough to hold the screen firmly then they tended to warp the chopper barrel, causing the Teflon plunger to hang up on its sides or to touch the coil itself. Although we improved the noise related to the screens considerably, we could not eliminate screen motion as one possible cause of the baseline drift, and it almost certainly contributed to the 100-count random noise, which corresponds to 0.3 microinch variations in the displacements of the screens.

Metallic Crankshaft--We also hypothesized that the metallic crankshaft could modulate the small amount of magnetic field leaking through the slot in the lower screen for the connecting rod to the plunger. In order to test this hypothesis, we operated the chopper motor and crankshaft with the connecting rod disconnected from the crank. In this configuration a relatively constant offset of 1 300 counts appeared, indicating that the crank could modulate about 0.08 ppm of the field. This value was not inconsistent with the fact that a screwdriver placed in the region of the crank caused a frequency shift of less than 0.1 ppm.

Under these conditions the baseline exhibited an rms noise of about 50 counts, and once in a one-hour run jumped by about 250 counts. This 500% jump could have resulted from a change in the shielding provided by the lower screen or from a 3-step (5.4-degree) variation in the motor synchronization, which was running open loop. Thus, the crank was not the primary cause of the baseline drifts and noise, although it did produce effects that had to be eliminated. It was expected that these effects could be reduced by improving the shielding between the crank and the coil, securing this shield more rigidly, and insuring that the motor was properly synchronized. Preferably, the plunger should be driven through a small round hole instead of the large slot necessary to pass a connecting rod. A linear drive for the plunger as provided by a cam-and-rod configuration would probably remove this offset entirely.

Conclusion--Although screen motion and the metallic crankshaft contributed to the noise and baseline drift, the motion of the Teflon plunger bearing on the chopper barrel appeared to be the principal source of the baseline drift.

#### 4.2.5.1 Effects of Motion of Teflon Plunger on Baseline Drift and Noise Level

The Teflon plunger bearing on the chopper barrel on both the up and down stroke caused modulation of the coil and movement of the oscillator circuit board, resulting in considerable noise and baseline drift.

Clearly two things not yet considered can move and therefore could have caused large effects on noise and baseline drift; namely, the coil itself and critical components on the oscillator circuit board. If this motion were repeatable for successive operations of the chopper, then a synchronously-modulated signal of constant amplitude would have resulted and would have produced a constant offset of the baseline, which could be removed by electronic means. However, the drifting baseline that was observed implied that the magnitude of this synchronous motion changed slowly with time as the chopper operated.

A possible source of this type of motion resulted from using a crank-wristpin drive for the plunger. It is inherent in this type of drive that the plunger must bear upon one side of the chopper barrel on the up stroke and then on the other side during the down stroke. The magnitude of the radial component of force depends on the angle between the connecting rod and the vertical and thus causes small deflections of the chopper barrel which are synchronous with the chopper motion.

Because only friction held the three-legged Teflon coil block in the center of the barrel, it was not difficult to imagine that the deflections of the barrel caused the coil to move back and forth about its nominal position. A 1-ppm modulation in inductance of this form would have caused a 17 000-count offset

in the baseline. If the magnitude of this displacement changed at an average rate rate of 0.7% per 12-s sampling interval as a result of slippage or Teflon coldflow, it would have caused the observed baseline drift of 600 counts/min. If this effect had been caused by friction-controlled slippage, we would not have expected it to be uniform in time but rather to have occurred in spurts, whereas coldflow would have been expected to be rather constant.

Both effects appeared present in the measured data in that sudden jumps between 500 and 2 000 counts were superimposed on the 600 counts/min. average drift. Teflon shavings found in the vent holes in the barrel added evidence that the plunger was bearing on the sides of the barrel.

We could estimate the coil motion required to produce a 1-ppm inductance shift by observing that the barrel reduced the inductance of the coil by about 10%. Thus, motion of the coil of about 15 microinch in the 1.5-inch-diameter barrel in synchronism with the motion of the plunger would cause a sufficient change in inductance to account for a 17 000-count offset. The baseline drift could then be explained by a change in this modulation of 0.1 microinch per 12-second sample. This modulation and drift rate did not appear inconsistent with the materials involved and the drive mechanism, and clearly could continue for many hours before being constrained or reversed.

Thus, it appeared essential that the plunger no longer be permitted to bear upon the barrel which shields the coil. Any necessary radial components of force would have to be absorbed by bearings outside of the chopper barrel and isolated from it. A Teflon or Vespel rod would have to be constrained to drive the plunger in a purely linear fashion with sufficient clearance and correct tolerances to insure that the plunger touched neither the barrel nor the coil at any time during its motion. Finally, the coil would have to be mounted to the barrel in such a way that it could not wander about. To prevent relative motion between the coil holder and barrel, the three arms of the coil holder would have to be pinned with considerable force. (A nonsynchronous slow creep of the Teflon caused by coldflow is no worse than a slow temperature change and thus would not be particularly serious. Its variations of the amplitude of motions which are synchronous with the motion of the plunger which must be totally avoided.)

The oscillator mounting also appeared to be a source of excessive random noise in the MOD I configuration and may also have contributed to the baseline drifts. The oscillator mounting also appeared to be a source of excessive random noise in the MOD I configuration and may also have contributed to the baseline drifts. The oscillator circuit board therefore was not mounted rigidly to the chopper barrel but to a copper shield, which in turn was glued to the crankhousing. In addition, the shield around the oscillator was not tight, and enough field leakage occurred in some configurations to cause frequency shifts approaching 100 Hz, depending on the placement of the outer shield. Also, it is possible that sensitive components associated with the tank circuit, such as the wires from the measure coil and the coupling transformer, may have vibrated synchronously with the chopper motion, adding to offsets and baseline drifts. The output and power cables freely suspended from the end of the oscillator box added to these mechanical instabilities.

These oscillator-related drifts and noise sources should also be removed by increased mechanical rigidity. The circuit components would ideally be in the

form of a hybrid integrated circuit. The oscillator mounting should be an integral part of the housing.

Conclusion--The analyses of the MOD I test results indicated many areas where changes could be made to substantially reduce the noise and drift. The chopper-oscillator assembly was redesigned to incorporate as many of these changes as possible in a breadboard-type assembly. The MOD II unit was then tested to determine the extent of improvement resulting from the changes. Test results for the MOD II unit are given in the following pages.

#### 4.3 Functional Tests (MOD II)

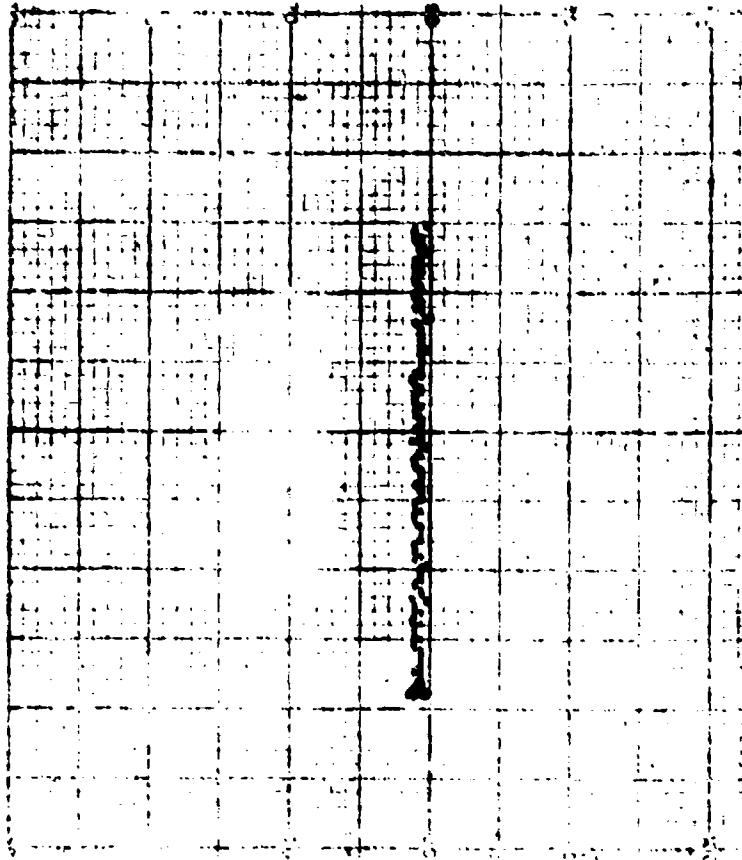
##### 4.3.1 Overall Performance of the MOD II

The MOD II tests show a dramatic improvement in performance over those of MOD I. The results support our conclusion that mechanical instability and vibrations were the major problems with MOD I. Further improvements can be made in known areas with a high probability of meeting all performance requirements.

Performance Summary--MOD II is a completely new mechanical design, including the substitution of Vespel for the Teflon chopper. When testing was started on the new assembly, output was erratic with full-scale noise. It was then realized that the Aquadag coating had not been applied to the Vespel chopper. When this was done, the noise level immediately dropped. At times, when sensing room air, the system noise did not exceed the electronic noise with the chopper stopped (see Figure 18). This would permit resolution approaching 1% of oxygen! Further, the output did not drift more than 2% oxygen equivalent during operation over a 10-hour period. A section of recording typical of this performance is shown in Figure 19. These results are indeed dramatic proof that our assessment of the MOD I problems was correct and, further, that with continued development the system should meet all the accuracy and stability requirements.

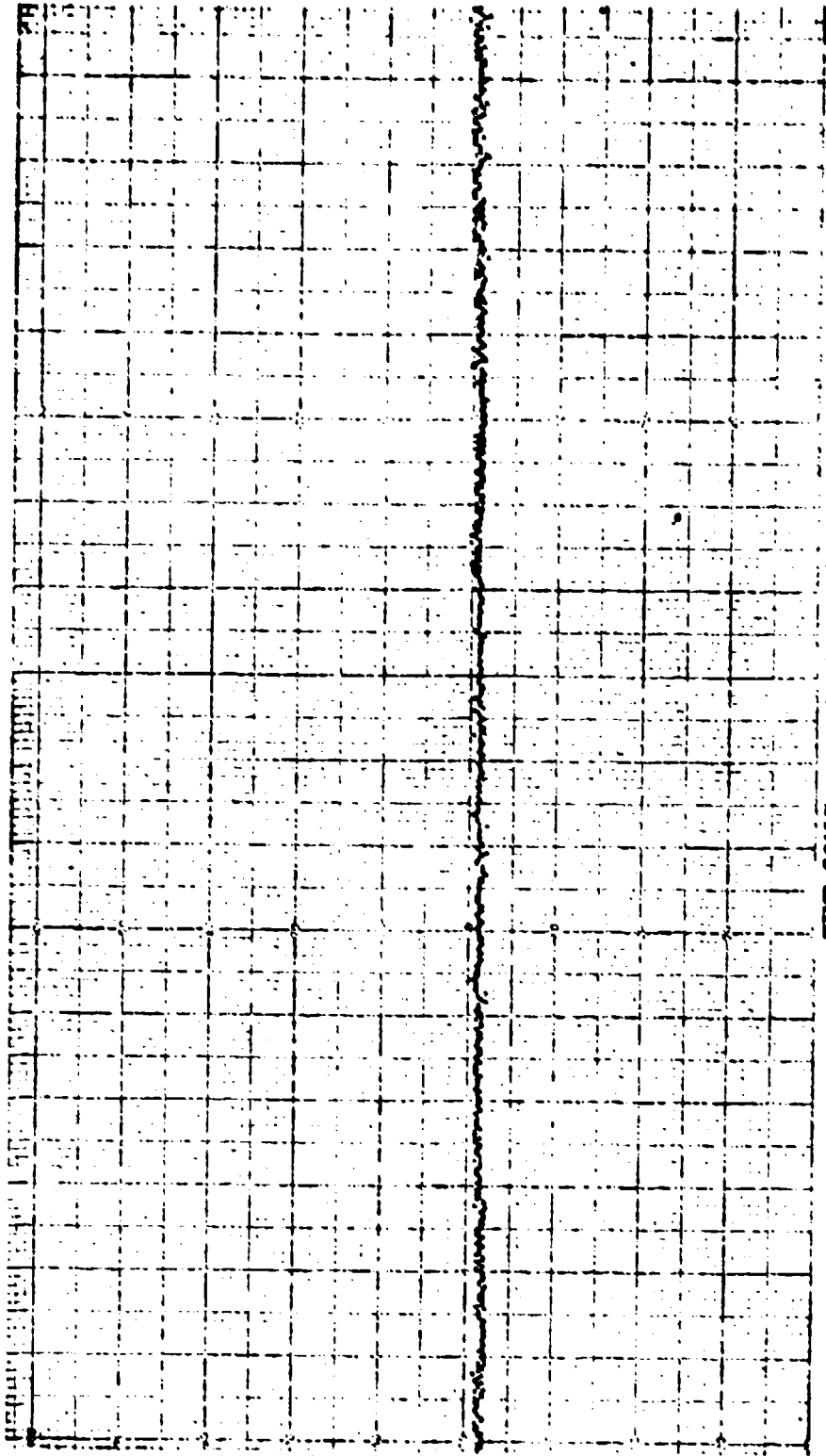
Noise Level Problems--However, problems still exist with MOD II as evidenced by a gradual increase in the noise level. After 16 hours of operation (overnight) the noise had increased to about 10% oxygen equivalent, but without any significant drift from the atmospheric oxygen baseline. As noted in the subsection on electronic design (3.2.2), any drift in frequency of the free-running measure oscillator will change the beat frequency from the crystal oscillator. The low-pass filter has a very narrow bandpass and a shift from the 22.2 kHz difference frequency will cause an increase in noise. Manual tuning of the crystal oscillator (a frequency synthesizer in this case) is then necessary to regain the 22.2 kHz beat frequency and maximize the signal through the filter. However, in this case peaking the signal only decreased the noise to 4 to 5% oxygen equivalent. This indicated an additional noise source or sources existed.

On rapping on the sensor housing, the noise level jumped to 25 to 30% oxygen reading and output became erratic. The system was examined thoroughly to determine whether parts had loosened or were defective. A bare wire located in the logic electronics was discovered to be lightly contacting the chassis cover. This was a major contributor to the problem, but others still existed after two days of probing. The noise level remained slightly above that which existed during the first day of testing.



TIME SCALE: 0 - 1 min.

Figure 18. MOD II—Electronic Noise Only  
(Chopper Off)



TIME SCALE:  $c = 1 \text{ min.}$

Figure 19. MOD II--Stability Test Measuring Roca Air

#### 4.3.2 Detail Results and Interpretation of Gas Sample Tests

A 2-1/2-hour continuous test of MOD II showed excellent repeatability and stability in its response to various gases and concentrations of oxygen.

Gas Sample Test--A test was made with a series of gas samples to show the response to carbon dioxide, nitrogen, propane, and varying oxygen concentrations. These tests were all made at ambient laboratory temperature and pressure. The results are shown on the chart in Figure 20. The chart covers about 2-1/2 hours of operation. The repeatability and stability can be seen to be excellent. The response between nitrogen and air (21% O<sub>2</sub>, 79% N<sub>2</sub>) is about 18 chart divisions with the D/A converter in a X1 mode. This is approximately the same level of output as for the MOD I unit. It is only about 36% of the theoretical response which would give 50 divisions for a 21% change in oxygen concentration.

Interpretation of Strip Chart Recording--There are several reasons for the less than theoretical output. The major ones are the low Q of the coil, flux leakage, and less than 100% chopping of the sample volume. With the noise level of about 2% oxygen equivalent observed during the last sampling tests, a factor of two increase in signal would permit measurements approaching 1% of true value. If the system noise level had been as low as recorded during the early testing (see Figure 18), then the increased signal would have provided performance very nearly meeting the ultimate requirement. We feel a factor of two increase in signal is practical to achieve.

A brief run was made with the D/A converter in the X2 mode. It can be seen that this improves the resolution of the measurement, as the noise is not amplified by a factor of two. This is because the system is not analog based. However, because of the statistical manner in which the data are handled, if the noise exceeds a certain number of counts it then is more visible as a spike on the X2 scale.

The relative response to the different gases is the same as found with MOD I. Nitrogen and carbon dioxide have a similar response, whereas 5% oxygen in nitrogen is clearly measurable. The output is linearly proportional to oxygen concentration (really partial pressure) in accordance with theory. Propane appears more diamagnetic than nitrogen, with about 5 chart divisions greater change from the room air baseline. However, sample data are available to prove this is not true; it is only -1% compared to oxygen at 100%. Therefore, we should only see about the same change as with nitrogen, which is -0.6%.

The reason for the observed result is that the propane is supplied from a storage bottle where it is contained as a liquid under about 100 psi pressure. Its evaporation causes a large temperature drop. The sample flow rate was 2 000 cc/min. through about 5 feet of plastic tubing. Without a heat exchanger to warm the propane, it caused a thermal transient in excess of the allowable 1°C per 100 seconds. With the sensing coil and electronics in a thermally controlled zone and adequate sample conditioning, no difference in response between propane and nitrogen should be seen.

A 5-minute run with 100% oxygen was made. The zero position was shifted in order to keep the reading on the chart. It is interesting to note the low noise level of this measurement. Again, the response is seen to be linear.

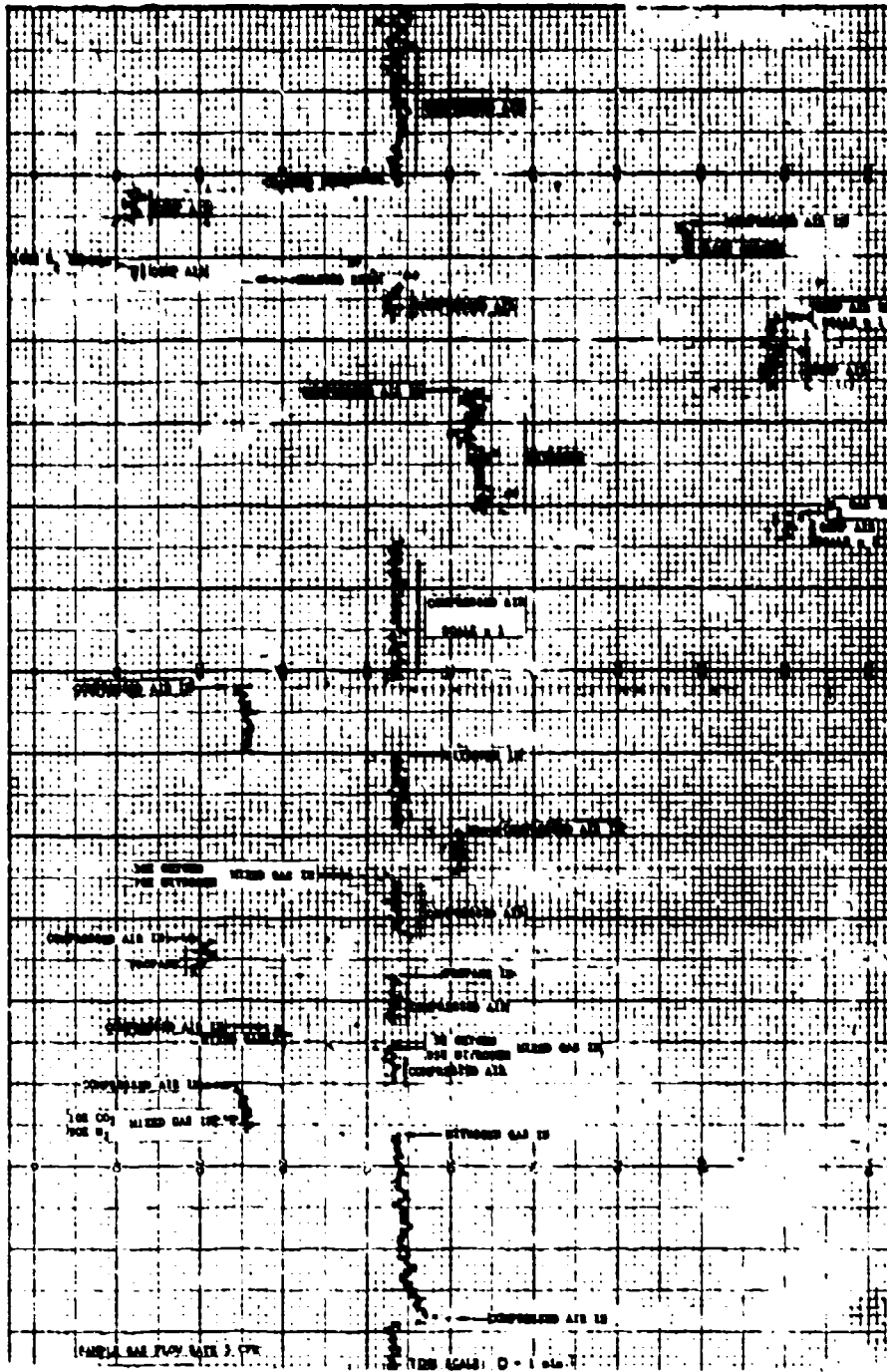


Figure 20. MOD II--Response to Cycled Sample Gas

Conclusions--Although tests with the MOD II unit were brief, the data are conclusive in showing that this concept is indeed feasible, and we have high confidence that it could be developed to a practical level.

## 5.0 CONCLUSIONS AND RECOMMENDATIONS

### 5.1 Discussion of Recommended Development Program

Based on the demonstrated capability of the breadboard, and particularly in view of the significant improvement between MOD I and MOD II, we believe further development of this concept is most desirable.

- Step One

As a first step in continuing development, we suggest additional testing with MOD II. This system can withstand temperatures up to 125°C; however, tests thus far have been limited to room temperature. Based on the known availability of components for 170°C operation, MOD II performance at 125°C would provide valid data for predicting 170°C results.

With the addition of the frequency control circuitry (phase-locked loop), long-term operating characteristics could be assessed. With the implementation of thermal control, sample conditioning, potting, and rigidizing of the electronics as well as a continued debugging, the ultimate accuracy and stability of the electronics could be closely approached.

- Step Two

Assuming favorable results from this first step, we suggest next going to an engineering model. This would incorporate the improvements from the MOD II tests into a unit configured for fuel-tank installation. After completion of tests with the engineering model to verify the acceptability of the design, a production prototype would be fabricated. This unit would be used for final qualification tests to assure full compliance with all flight operational requirements.